HYDROLOGIC DRIVERS OF NITROGEN CYCLING: IMPLICATIONS FOR AN EARTH SYSTEM MODEL AND AGRICULTURAL MANAGEMENT PRACTICES

A Dissertation
Presented to the Faculty of the Graduate School
of Cornell University
In Partial Fulfillment of the Requirements for the Degree of
Doctor of Philosophy

by
Chelsea Kimberly Morris
May 2019

HYDROLOGIC DRIVERS OF NITROGEN CYCLING: IMPLICATIONS FOR AN EARTH SYSTEM MODEL AND AGRICULTURAL MANAGEMENT PRACTICES

Chelsea Kimberly Morris, Ph. D.
Cornell University 2019

The research in this dissertation is broadly concerned with the measurement, modeling, and management of nitrogen transport and transformation in agricultural watersheds. Our objective in the first study was to quantify nitrogen losses under different cover crop treatments to provide insights into the environmental benefits of cover crops over their lifetime. We measured nitrous oxide emissions, nitrate leaching, and plant nitrogen demand in the early spring and continued nitrous oxide measurements after tillage. We found the environmental benefit of cover crops depends on the type and period of analysis. Legumes increased nitrous oxide emissions to the atmosphere post-tillage over the non-legumes. Neither legume nor non-legume, nor a mixture of the two, was effective at reducing nitrous oxide during the growth phase relative to fallow conditions.

In the second study, we examined the scale-dependency of several nitrogen cycle processes in an earth system model with previously identified scale issues in its hydrologic cycle and recognized difficulty in simulating gaseous and hydrologic-driven nitrogen losses. We

hypothesized that observed discrepancies in these soil nitrogen processes across grid-scales are explained by issues in hydrologic scale-dependence. The recommended spin-up procedure generated different soil hydraulic properties for a model resolution, resulting in different drainage and runoff rates. We confirmed that the choice in grid scale affected model estimates of soil moisture, nitrification, nitrate leaching, and to a lesser degree, denitrification.

In the final study, we present an exploration of flow variability and denitrifying bioreactor performance that aim to improve management of nitrogen in tile drainage water. Using synthetic data modeled after observed flow distributions in an existing bioreactor in central New York, we found that a record with a few high flow events generated greater nitrate export than a record with frequent low flow events. The finding supports the general design practice of building the reactor with appropriate size and flow control to maintain a low flow rate.

BIOGRAPHICAL SKETCH

Chelsea Morris grew up in Pennsylvania, Illinois, and Oregon but now calls anywhere with her copious plant collection home. Prior to beginning her doctoral research at Cornell University, she completed a master's degree in the same department and an undergraduate degree in Civil & Environmental Engineering at Tufts University. Her undergraduate design project, an anaerobic digester for a Vermont dairy farm, was the beginning of her deep enthusiasm for agricultural nutrient cycling and water quality protection. Between undergraduate and graduate school, Chelsea learned to drive a tractor poorly, parallel park a box truck in downtown Boston, and write technical briefings for the US Environmental Protection Agency. After completing her work at Cornell University, Chelsea is heading back to government to work on nutrient management in animal agriculture.

ACKNOWLEDGMENTS

This dissertation should have many authors, I sincerely believe this. It wasn't a singular herculean effort on my part that got these words on paper, but a community of supporters, critics, providers, and advisors who contributed to the work. I begin my thanks with the Ithaca community who saw me through the day to day—thank you Patty and Ian for the constancy of your humor and patience. You melt me. For beautiful advice and pointing me to lightheartedness, I appreciate you Jaya and Laura. Thank you Caitlin for the food you prepared and community you tied together every week. To Jess, thank you for never being afraid of the dark.

Mom and Dad, I love that you instilled this curiosity in me, Trey, and Jenna. It's enriched my life more than any afterschool program. Thank you Mom for helping me design and execute my very first water quality project in the Schuylkill River and for being a tireless cheerleader. Dad, your steady support and has made all of this possible. I feel so lucky to have you both as parents.

To my Cornell mentors and colleagues – Ty, Sara, Emily, Will, Erin, Lisa, Christine, Allison, Brian—I have endless appreciation. You were there to question the way of things, willing listen to my struggles and rants, and committed to building a better place. Thank you for the inspiration to explore bigger concepts in academia than this dissertation. Lauren, you lead by example and showed me the fun in scientific collaborations. For Sheila, my dear deskmate and confidant, and James, the incredibly kind whiz kid, I am undone with gratitude.

To Owen who sent encouragement from afar and helped me battle imposter syndrome, I love the research video you made for me. You make every scientist you talk to feel like a million bucks.

My committee members Christy and Matt, you had such patience for me in my final years as I worked in fits and spurts while suffering from deep doubt. I asked you to be on my committee because I valued your integrity and scientific mind. It was an absolute honor to work with you.

And lastly, I extend a deep bow of thanks to Todd. Thank you for making and fostering this space for me to grow intellectually and emotionally. I appreciate that you so valued a flexible, human-centered, academic environment and gave us a lab that wasn't perfect, but so collaborative in its imperfection.

TABLE OF CONTENTS

CHAPTER 1
A COMPARISON OF NITROGEN LOSSES FROM COVER CROPPED FIELDS UNDER GROWTH AND POST-TILLAGE

Introduction

In the early spring in the Northeastern United States, as snow melts and soils thaw, the region experiences a flushing of reactive nitrogen (N) into the hydrosphere and atmosphere (Sebestyen et al., 2008; van Bochove et al., 1996). Soils become saturated with snowmelt water and spring rains, mobilizing N from soil and stimulating the biological N cycle. The N released to air and water from fertilized agricultural lands is particularly extraordinary (Wagner-Riddle et al., 1997). High concentrations of nitrate in groundwater and surface waters pose risks to human health and aquatic ecosystems (Erisman et al., 2013). Gaseous losses of the powerful greenhouse gas nitrous oxide (N_2O) contribute to the overall change in global climate (World Meteorological Organization, 2016). Much of the anthropogenic N_2O comes from agricultural soils, and more than half of annual agricultural N_2O emissions occur in the early spring (Wagner-Riddle et al., 2017).

Concern for aquatic ecosystem health and global climate has led to the development of agricultural strategies to manipulate N cycling in the field. Ideally, N fertilizer is applied at agronomically appropriate rates, using methods that minimize losses at times when the fertilizer is most needed. Still, targeted application fails to prevent N losses in all situations (Christianson & R. D. Harmel, 2015). There is a need for strategies that promote N retention in agricultural soils. Ideally, such a strategy holds N in place for use during the next growing season, thus reducing the need for future fertilizer applications.

Cover crops (CCs), planted after a cash crop, are one such strategy that can hold onto the excess soil N. CCs scavenge nutrients, drawing water and N into plant tissue that would otherwise leach out of the soil profile (Meisinger et al., 1991). Meta-analyses indicate that CCs regularly reduce leaching across climates and cropping systems (Tonitto et al., 2006), but their ability to reduce N_2O emissions is less certain (Basche et al., 2014, Han et al., 2017). Nitrification and denitrification are the two soil N cycle processes that produce the majority of N_2O in row crop agriculture. These two processes are linked, in that nitrification converts ammonium to nitrate (NO_3), which is the reactant necessary for denitrification. The type of CC should affect both hydrologic and gaseous N losses. Legume CCs derive a portion of their N requirements through fixation conducted by soil microbes. Non-legume CCs rely on the existing soil N pool for most of their nutrient needs. As a result, non-legumes have a greater demand for soil N than legumes, which influences the magnitude of N losses during CC growth. Under high soil N conditions, legumes reduce their fixation rates and fulfill a larger portion of their necessary N from the soil (Hardarson & Atkins, 2003). Correspondingly, soils planted with legumes are reported as having higher N_2O emissions when less fertilizer N is applied than those receiving more fertilizer N (Basche et al., 2014, Han et al., 2017).

We tested two common CC monocultures, vetch (legume) and wheat (non-legume), and a biculture of the two (referred to as a mixture), for their relative performance in minimizing N losses during growth and following tillage (before planting the primary crop). N cycling under CCs can be considered according to their life cycle from planting to cessation by tillage prior to cash crop planting. In this study, we compared the cumulative N_2O production between CC types for two

management periods: during the CC growing period, and in its post-tillage period.

During the CC growing period, plants compete with soil microbes for soil inorganic N. Different CC types have different N demands, based in part on the plant's access to fixed N. We expect wheat to outcompete vetch for soil N and thus have lower N_2O emissions during the growing period. Once killed and incorporated into the soil, CC residue releases N back to the soil and ideally will be taken up by the newly planted cash crop. The rate and timing of N release from CC residue is dependent on the C:N ratio of the plant tissue, soil moisture content, and temperature (Wagger et al., 1998). We expect vetch to release N to the soil more quickly and produce more N_2O than wheat before the cash crop is planted. Environmental conditions that control N losses vary under different CC types as well. Warmer conditions increase the microbial activity of both nitrification and denitrification. Wetter soil conditions increase the transport of inorganic N and create the anoxic environment necessary for denitrification. CCs alter these environmental conditions through soil surface shading and transpiration. We investigate whether the CCs alter these environmental conditions and whether these changes are large enough to alter N losses.

Our objective in this study is to quantify N losses under different CC treatments to provide insights into the environmental benefits of CCs over their lifetime. We measured N_2O emissions, nitrate leaching, and plant N demand in the early spring and continued N_2O measurements after tillage.

Methods

Winter CCs were planted in September 2014 at Musgrave Research Farm in Aurora, New York where corn, soybean, and hay are grown in rotation according

to research needs. The 2014-2015 winter and spring was cooler and wetter than the 30-year normal for Aurora, New York (Northeast Regional Climate Center, 2018). Mean monthly temperature in the winter months was -7°C, colder than the average of -3°C. Spring and early summer temperatures were also cooler than average, but not as drastically as during the winter. The farm received 0.60 m of precipitation during the study period compared to an average of 0.64 m. The soils at the farm are a cobbly loam formed in glacial till and tile-drained. Four replicates of the three treatments (vetch, wheat, and a mixture) and fallow control plots were prepared in a randomized design. Walking paths (3 m wide) between the planted plots (12 m^2 area) were set directly over the tile-drainage line such that drainage in the plots was affected relatively similarly across the treatments. Hairy vetch (*Vicia villosa Roth*, Albert Lea) was planted as the N-fixing legume and winter wheat (*Triticum aestivum*, Houser) as the non-legume grass. Plots containing both vetch and wheat were planted as an equal mixture by seed count. Plots were divided, with half receiving no fertilizer and the other half receiving ammonium-nitrate fertilizer (24-0-0) on 6 May 2015 at a rate of 224 kg NH_4-NO_3 ha^{-1}. On 15 June 2015, all plots – including fallow soils – were hand-tilled.

Nitrous Oxide Emissions

Trace gas fluxes were measured using the static gas chamber method (Hutchinson and Mosier, 1981) and gas chromatography. Chamber collars (27.4cm ID) made from 5-gallon paint buckets were inserted 5-8 cm into the soil in each of the 32 subplots in November of 2014 to ensure secure placement before the ground froze. Gas sampling began on 21 April 2015 and continued nearly biweekly for 5 measurements prior to tilling on 15 June. Gas emissions were then sampled six times over the two-week period after tillage.

At the time of gas sampling, a 5-cm wide rubber band was placed around the

outside of the collar and a white-opaque lid (27.4cm D x 34.4cm H) with a rubber septa and pressure equilibrium vent (Hutchinson and Mosier, 1981) was fitted on top. The thick rubber band ensured the chamber was sealed. Gas samples (15 mL) were drawn from the chamber through the rubber septa using a 20 mL syringe and injected into pre-evacuated 10 mL vials. Samples were taken at 10-minute intervals—at 0, 10, 20, and 30 minutes. Soil volumetric water content (Hydrosense, Campbell Scientific Inc.) and temperature (Marathon digital thermometer) measurements were taken near each collar after the sampling campaign was completed.

Samples were analyzed for carbon dioxide (CO_2) and N_2O using gas chromatography (Agilent 6890N with electron capture detector and flame ionization detector). Fluxes were calculated using a linear regression of the change in gas concentrations over the four time points (Anthony et al., 1995). Seals on the gas collar and chamber set-up were checked by manually inspecting the CO_2 curves. Under a complete seal, CO_2 concentrations increase with time. Samples at time-points where the CO_2did not increase were assumed to be compromised and were removed from the dataset, and the linear flux was calculated from the remaining three points. On average, two time-points from each sampling campaign were removed, meaning a majority of the fluxes were calculated using four time-points. The minimum detectable flux for the analyzer was 25.4 ppm hr^{-1} (Parkin & Venterea, 2010).

Nitrate Leaching

Inorganic N (NO_3^-, NO_2^-, $NH4^+$) leaching was measured *in situ* with intact soil columns and ion exchange resins, installed on 29 April 2015 when CCs were less

than 15cm tall. The soil columns were incubated for six weeks and the plants continued to grow. Thirty-two columns were made from 45.7 cm-L x 7.6 cm-D PVC pipes (schedule 40). Two holes (1.25 cm D) were drilled 2.5cm from the top edge of the tubing to allow insertion of an aluminum rod-handle used to ease in removal of the column from the ground. The two holes also acted as drainage ports for surface runoff after installation. The bottom edges of the columns were lathed to a 30-degree angle to create a sharp edge for driving into the soil. Temporary aluminum caps were placed on the top of each column, which was then driven vertically into the ground by sledgehammer and by weighted twisting on the rod-handle. Once driven to a target depth of 40-44 cm, the column was removed by lifting the rod-handle. Soil remained intact inside the column during extraction and the plant on the soil surface was carefully handled. An additional 2.5 cm of soil was removed from the extracted column to provide room for an ion exchange resin pack (detailed below). Resin packs were placed at the base of each column against the soil surface, and were secured in place with rubber O-rings and nylon mesh screens that had been cut and sewn together to create a porous 'cap'. The pack was anchored to the PVC column with silicone caulk (GE Silicone 1, free of anti-microbial products) allowed to dry 10-20 minutes (until no longer tacky) before the columns were replaced in their associated holes. At four of the 32 plots (a fertilized mixture, unfertilized vetch, and two fertilized fallow plots), presence of rocks prevented installation of leaching columns.

The ion exchange resin packs were constructed of acid-washed nylon stockings and rubber O-rings. Thirty grams of mixed anion and cation exchange resin beads (Rexyn, Fischer Scientific) were placed in each sack and either tied shut or stapled with stainless steel staples. Resin packs were washed in a 1M solution of NaCl for 1 hour, then rinsed in deionized water and stored in plastic bags overnight. One

field blank resin pack was placed inside a plastic bag at the site to assess contamination prior to installation. A second blank pack was kept in a plastic bag in the laboratory.

Soil columns were removed on 15 June 2015, bagged, and brought back to the laboratory for analysis. The resin packs were removed, placed in individual plastic bags and refrigerated for 48 hours until extraction. Resin beads (~2 g wet-weight) were extracted with 40 mL (first round) then 20 mL (second round) of 2 M KCl later analyzed colormetrically for NO_3, nitrite and ammonium (Kjønaas, 1999a & 1999b; O'Dell, 1993; Bower & Holm-Hansen, 1980). The mass of inorganic N leached from the column was calculated by multiplying the mass of N per g of bead by the mass of the resin pack (30g) and divided by the surface area of the column and the incubation period, to yield an areal flux (g N $m^{-2}d^{-1}$).

Plant Nitrogen Demand

At the end of the growing period, aboveground plant biomass was assessed in each plot. The aboveground plant matter was removed from a section of each subplot and weeds were sorted from the CC. CC plant matter was dried, and weighed to determine biomass. A subsample of the plants collected for the plot biomass measurement were analyzed for C and N content (%) by combustion (LECO C and N analyzer, St. Joseph, MI, USA). The proportion and amount of vetch N fixed from atmosphere in the unfertilized plots was calculated using the ^{15}N natural abundance method from Shearer and Kohl (1986). See Reiss (2018) for collection and measurement procedures.

Statistical Analyses

Statistical analyses were conducted in R v. 3.3.2 (The R Project for Statistical

Computing, 2017). The N_2O fluxes were summed according to their location and time period (growing versus post-tillage) for all analyses. The Wilcoxon rank sum nonparametric test was used to assess N_2O differences between fallow and CC plots. Analysis of variance and post hoc Tukey test were used to determine difference between treatments in losses of N_2O and NO_3. Paired Wilcoxon rank sum tests were used to assess differences in losses of N_2O and NO_3 between fertilized and unfertilized treatments and differences in N_2O emissions between the growing and post-tillage periods.

Results

Peak N_2O fluxes occurred in the vetch plots, followed by the fallow plots (Figure 1). These peak fluxes occurred in the post-tillage period, 2 to 7 days after plants were incorporated. Cumulatively, the highest N_2O emissions occurred in the fertilized vetch plots during the post-tillage period (average 2.18 ng/m2/per day) and the fertilized fallow plots during the growing season (average 0.782 ng/m2/per day).

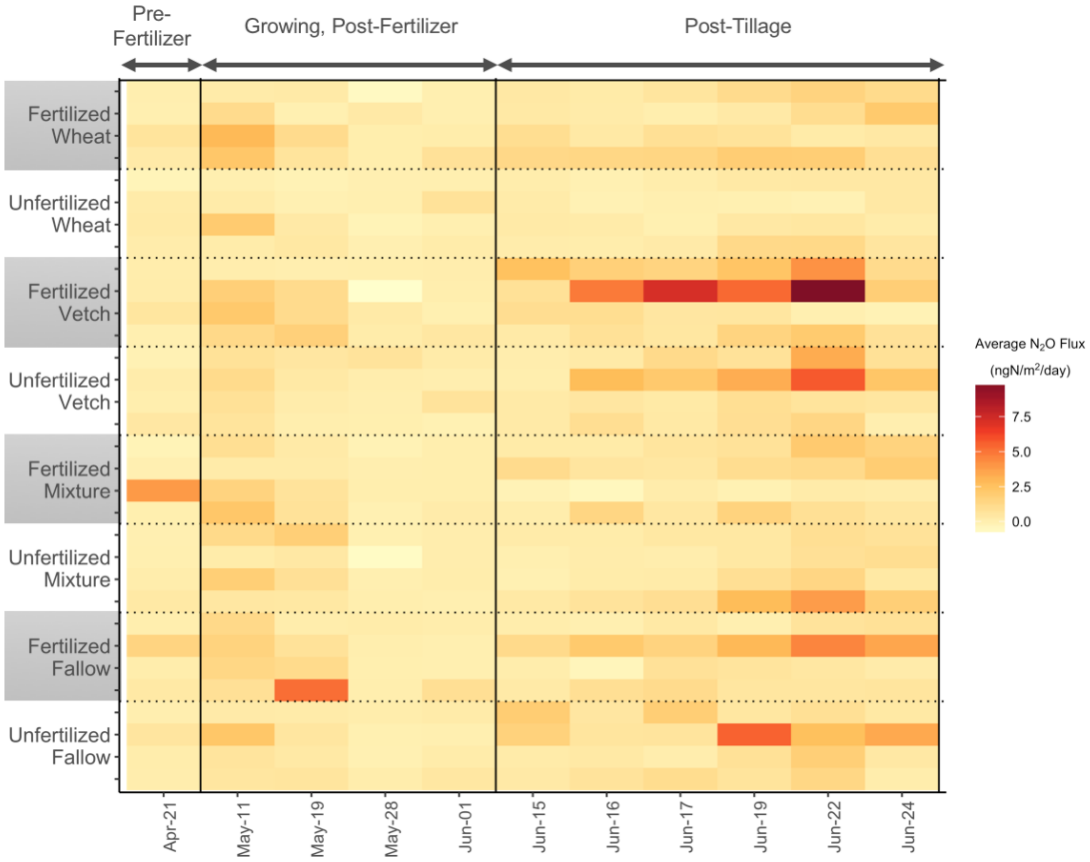

Figure 1 Nitrous oxide fluxes under CC and fallow fields from post-thaw to pre-planting. The vertical line between April 21 and May 11 separates the pre- and post-fertilizer periods. The second vertical line between June 1 and June 15 indicates when the plots were tilled and growing plants incorporated into the soil. The highest peak fluxes, indicated by a darker red color, occurred after CC were tilled.

The presence of a CC did not reduce total N_2O emissions over the entire measurement period (Figure 2A) and there were no significant differences within the CC treatments (Figure 2B). Instead, N_2O emissions were related to soil temperature (Figure 3, Figure 4, $P = 0.002$ $R2 = 0.24$). Soil temperature also correlated to aboveground biomass in the plot (Figure 5, $P = 0.0014$, $R2 = 0.35$), with cooler temperatures in plots with more biomass, however the direct relationship between aboveground biomass and cumulative N_2O emissions was not

significant (data not shown, P = 0.0955). Plots with higher mean soil moisture or greater variation did not have greater N_2O emissions (data not shown, P = 0.437 and P = 0.888).

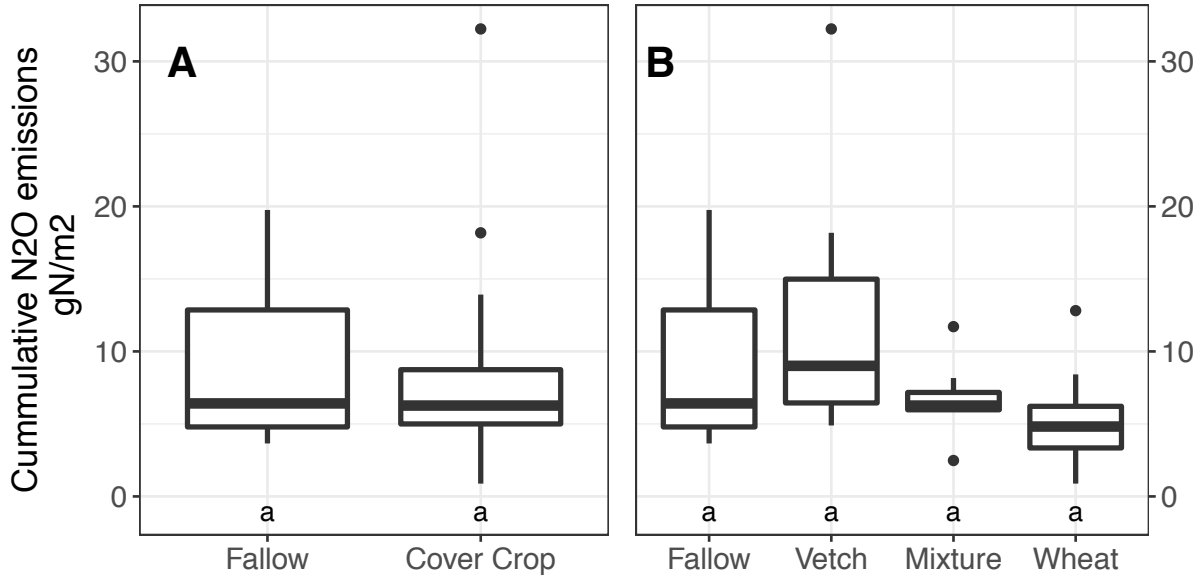

Figure 2 Cumulative nitrous oxide emissions across all measurement under fallow and cover cropped fields (A, n = 8, 24) and by cover crop type (B, n = 8, 8, 8, 8). Center lines show the medians. Box limits indicate the 25th and 75th percentiles, with whiskers extending 1.5 times the interquartile range. Outliers are represented by dots. Different letters under each boxed group indicate statistically significant differences in means.

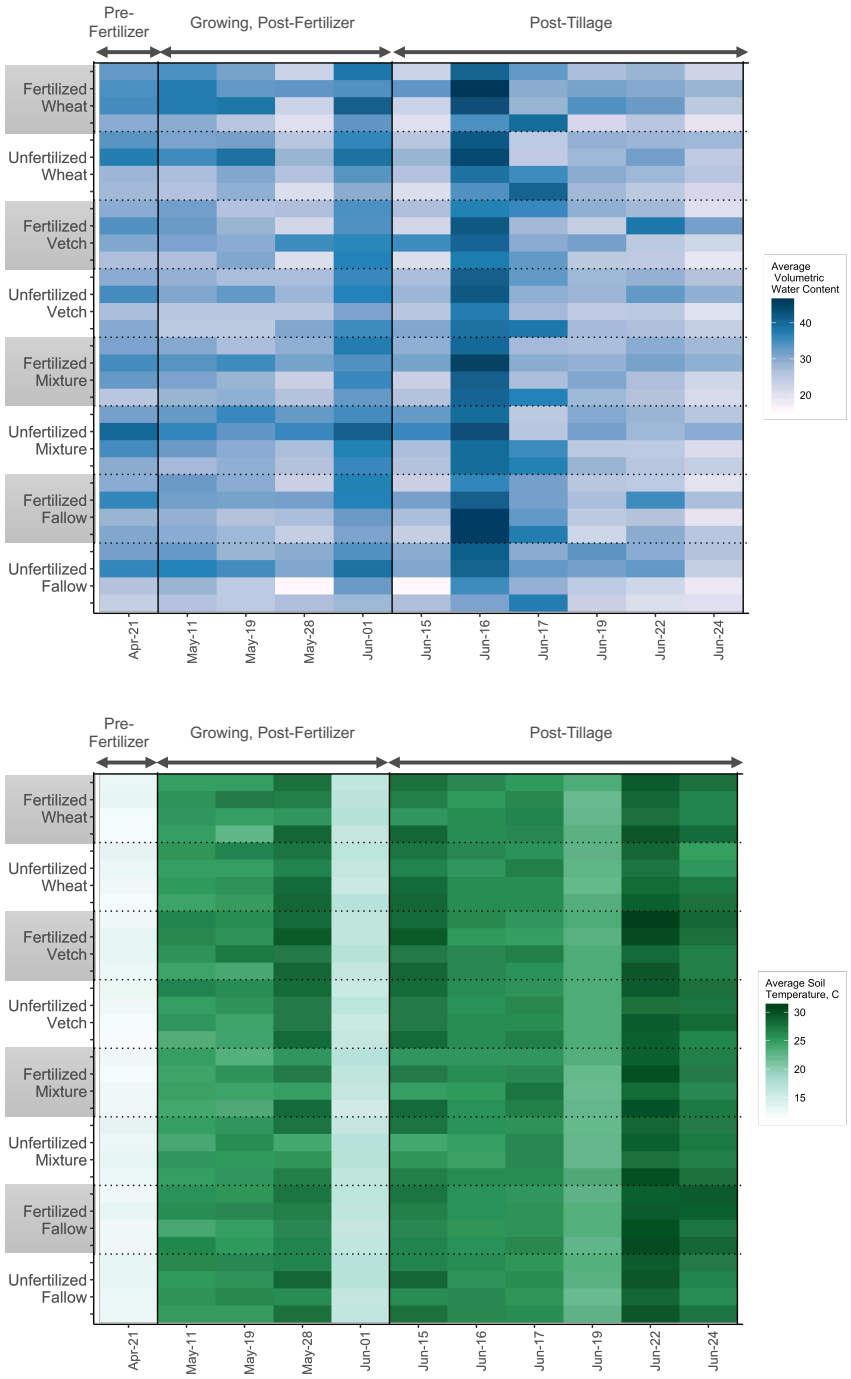

Figure 3 Soil moisture (above, in blue) and soil temperature (below, in green) observed near the gas chamber at the time of gas sampling. Within a day, soil moisture was more variable across the field than soil temperature. This heterogeneity contributes to the spatial heterogeneity in N_2O fluxes. The vertical lines separate the different measurement periods.

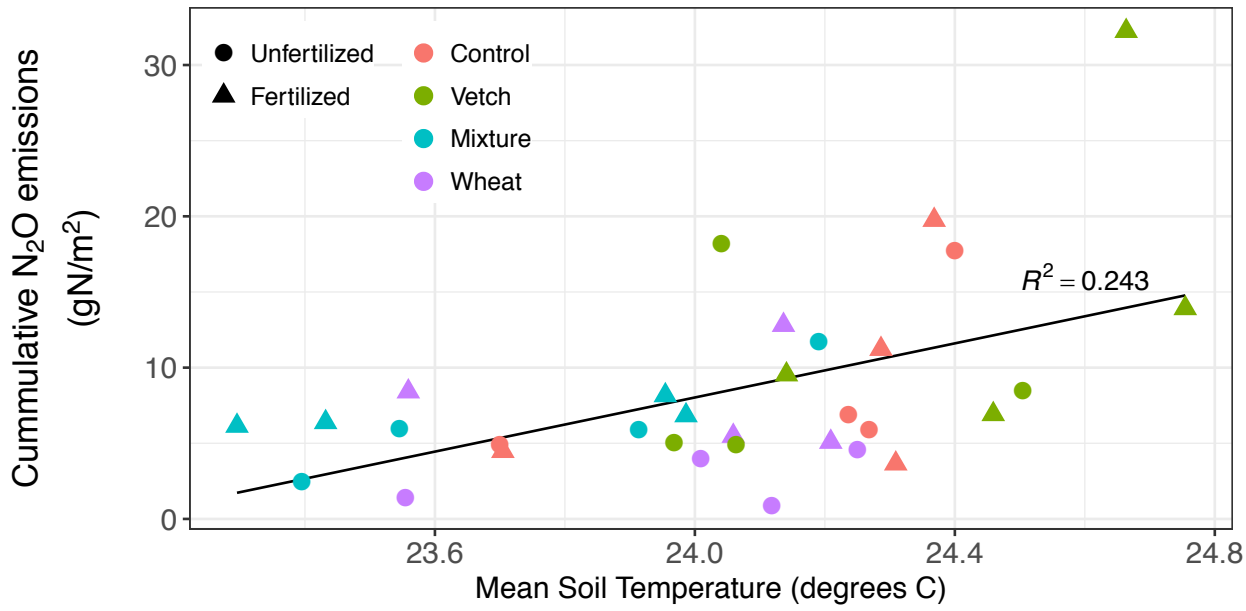

Figure 4 Cumulative nitrous oxide emissions versus mean soil temperature from entire measurement period. The black line shows the significant linear relationship.

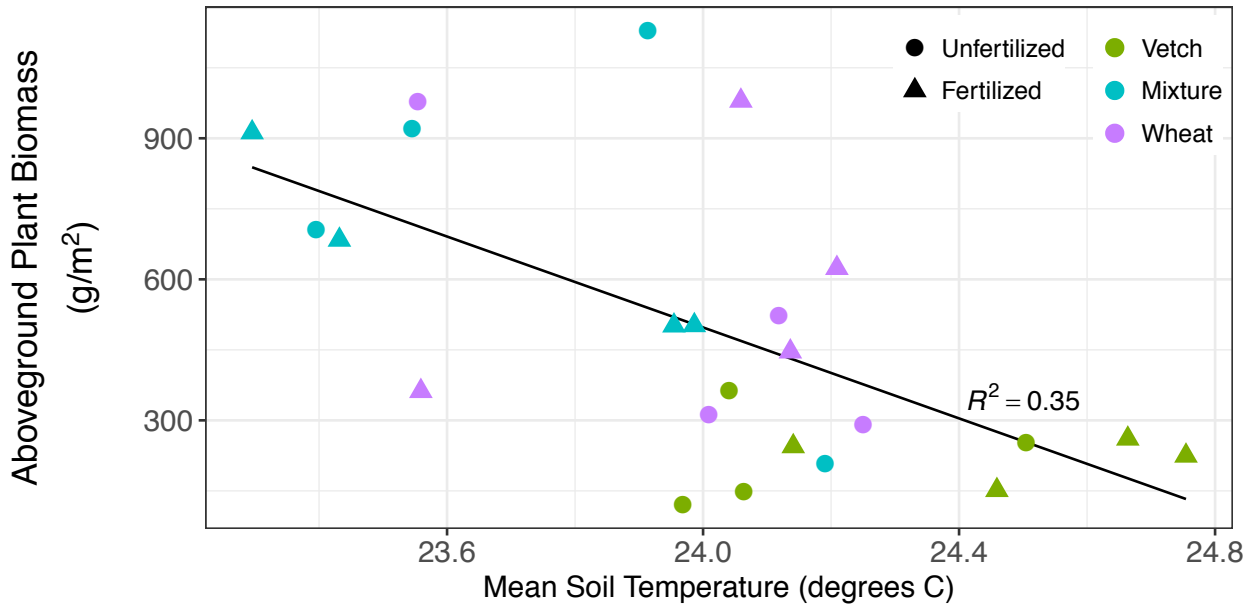

Figure 5 Aboveground plant biomass of the plot versus mean soil temperature for the entire period. The black line shows the significant linear relationship between the plant biomass and mean soil temperature in all plots.

Compared between the two observation periods, the CC produced significantly greater N_2O in the post-tillage period than in the growing period (Figure 6A, P = 0.004). However, vetch was the only CC in which the growing period N_2O emissions differed from the post-tillage period (Figure 6B, P = 0.02). N2O production from the fallow plots did not increase after tilling, but became more variable.

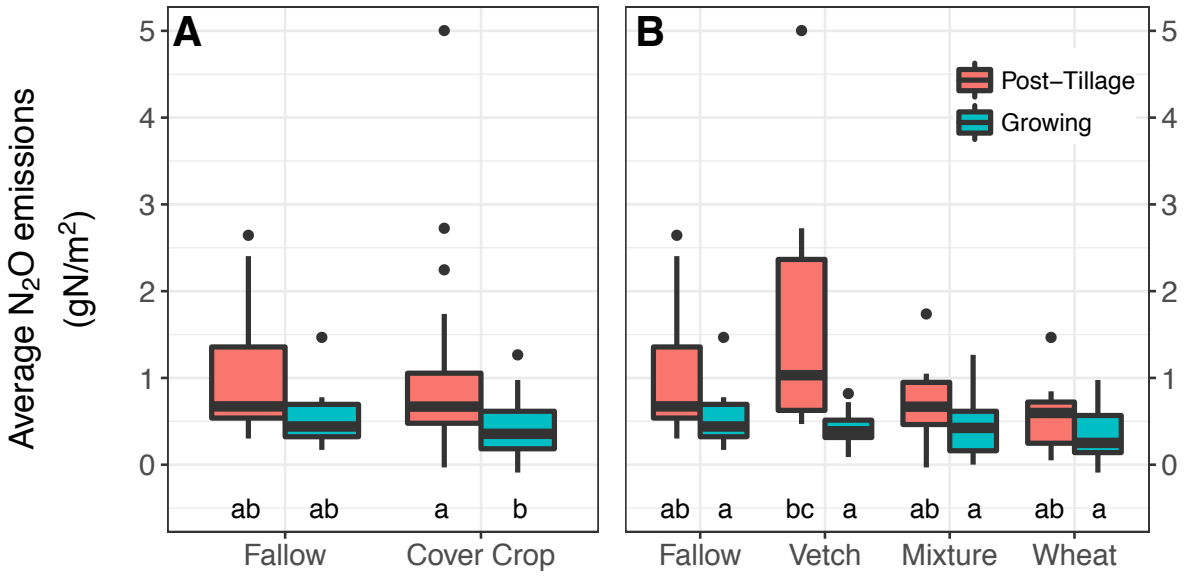

Figure 6 Average nitrous oxide emissions for each observation period under fallow and cover cropped fields (A, n = 8, 8, 24, 24) and broken out by cover crop type (B, n = 8 for all groups). Center lines show the medians. Box limits indicate the 25th and 75th percentiles, with whiskers extending 1.5 times the interquartile range. Outliers are represented by dots. Different letters under each boxed group indicate statistically significant differences in means.

While the presence of a CC did not significantly lower N_2O emissions during the growing period, CCs did decrease NO_3 leaching (Figure 7A, P = 0.003). Leaching from the mixture was significantly lower than fallow plots (Figure 7B, P = 0.02). Wheat was lower, but not significantly different from fallow, mixture, or vetch in part because of the low number of replicates (n=2). The extractable NO_3 concentration in the soil at the end of the growing period did not differ significantly under a CC or among types of CCs (data not shown).

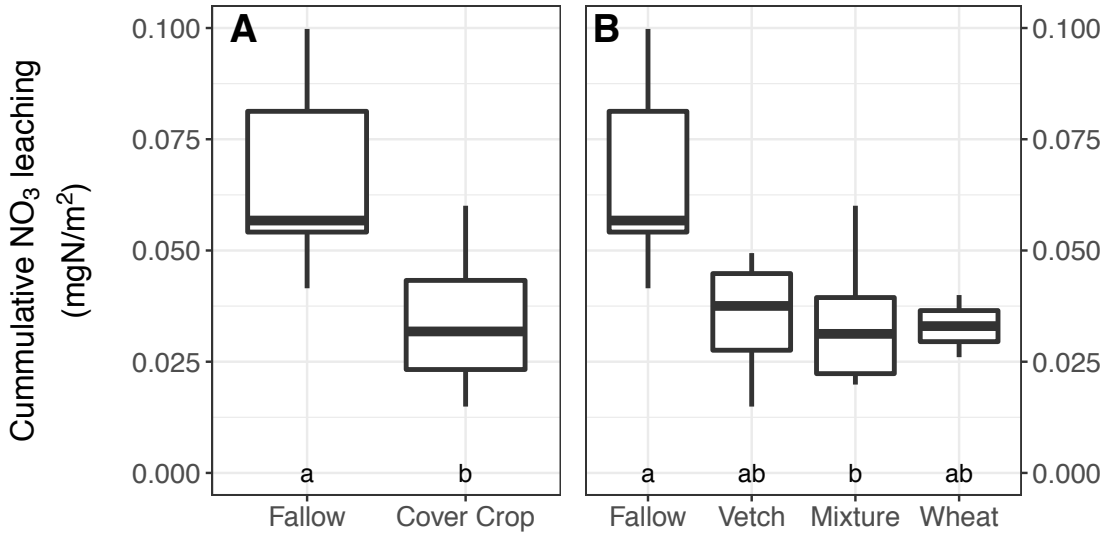

Figure 7 Cumulative nitrate leaching from fallow and cover cropped plots (A, n=6, 13) and broken down by cover crop type (B, n=6,4,7,2) during the growing period. Center lines show the medians. Box limits indicate the 25th and 75th percentiles, with whiskers extending 1.5 times the interquartile range. Outliers are represented by dots. Different letters under each boxed group indicate statistically significant differences in means.

We observed increases in N_2O losses when more N was available as fertilizer. Under fertilization, N_2O emissions increased when compared to paired unfertilized plots (Figure 8A and Figure 8B, $P = 0.009$). The largest N_2O increase in response to fertilization occurred in the wheat plots, although it was not statistically significant due to the small sample size (n=4 for each group). There were no differences in the amount of NO_3 leached from the fertilized plots (data not shown).

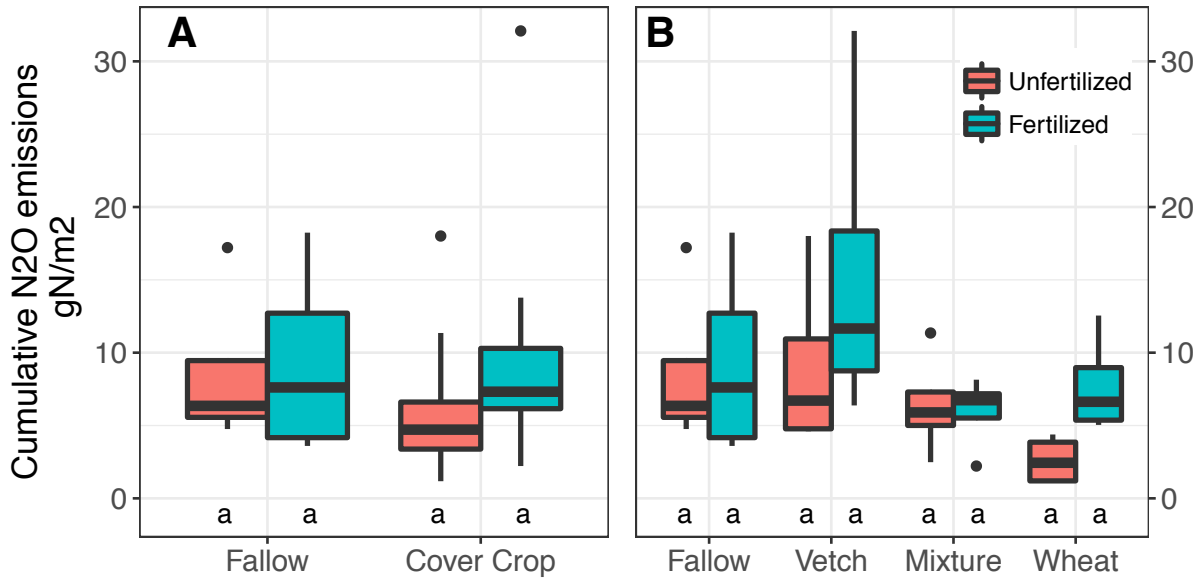

Figure 8 Cumulative nitrous oxide emissions by fertilizer status under fallow and cover cropped fields (A, n=4, 4, 12, 12) and broken out by cover crop type (B, n=4 in each group). Center lines show the medians. Box limits indicate the 25th and 75th percentiles, with whiskers extending 1.5 times the interquartile range. Outliers are represented by dots. Different letters under each boxed group indicate statistically significant differences in means. Although there are no significant differences between groups, in a paired plot analysis, fertilized treatments produced significantly more nitrous oxide than their unfertilized pair.

Plant N concentration correlated with N_2O emissions overall (Figure 9A, P = 0.0190, R^2 =0.943) and in the post-tillage period (Figure 9B, P = 0.046 R^2 =0.87), but not the growing phase (Figure 9C). Plant N content in the mixture did not correlate with N_2O emissions, however there was a slightly negative trend in the wheat plot N_2O emissions (Figure 9B, P = 0.1005, R^2 =0.714).

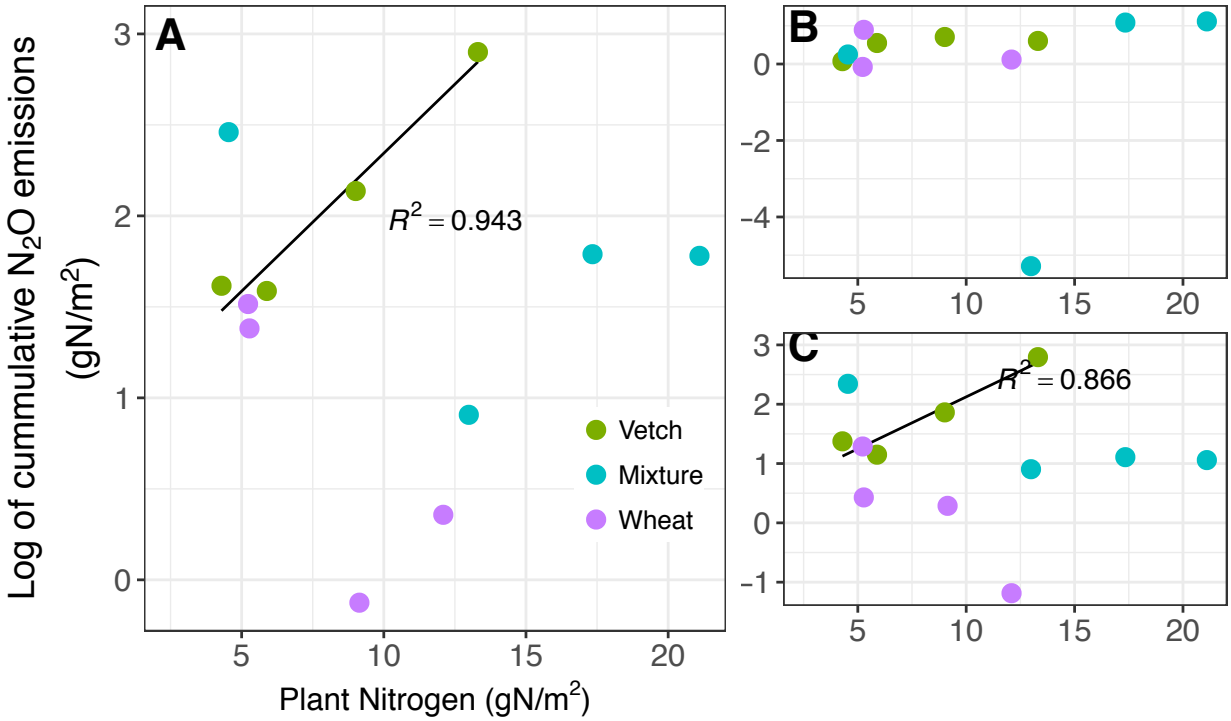

Figure 9 Lognormal cumulative nitrous oxide emissions compared to plant N concentration for the entire period (A), growing period (B), and post-tillage period (C). Data are from unfertilized plots. The black line shows the significant linear relationship between the cumulative N_2O emissions and plant N in the vetch plots.

Plant tissue stoichiometry, which often correlates with the rates of decomposition and denitrification, correlated with total N_2O emissions in the post-tillage period for all CC treatments (Figure 10, P = 0.00234, R2 =0.583). CCs with higher C:N ratios had significantly lower total N_2O emissions, although the negative linear trend was strongly determined by the four wheat observations.

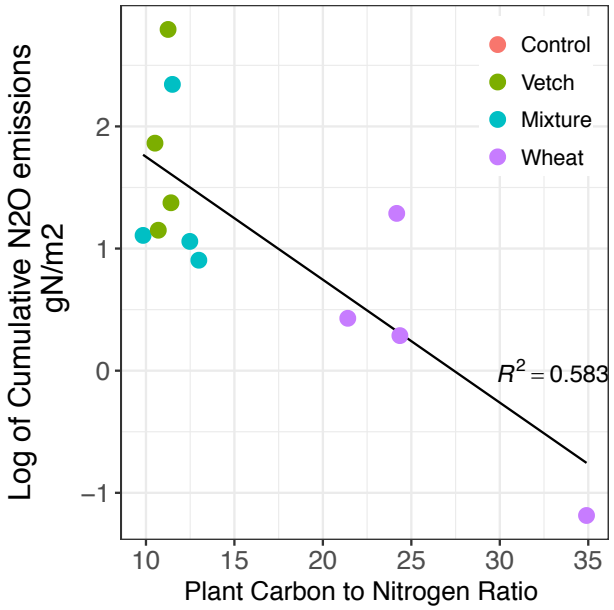

Figure 10 Cumulative nitrous oxide emissions during post-tillage period compared to plant carbon to nitrogen ratio. Data are from unfertilized plots. The black line shows the significant linear relationship between the N_2O emissions and C:N ratio in all plots.

Discussion

In both the CC growing period and post-tillage, we found the presence of a CC did not significantly impact N_2O emissions compared to a fallow field. Instead, N_2O emissions over the entire period corresponded to cross-plot differences in soil temperature and vetch N concentration. The negative relationship between aboveground biomass and soil temperature suggests the treatment effect is partially explained by the biomass differences of wheat and vetch. Wheat plots with a higher aboveground biomass were cooler on average due to shading than the low-biomass vetch plots. A similar soil temperature decrease created by biomass shading was reported by Sainju et al. (2012).

Given the significant differences in N_2O emissions post-tillage compared to the growing period, we frame the following discussion of the climate benefits of CCs

by observation period.

Nitrous Oxide Losses in the Growth Period

Wheat CCs were expected to reduce N_2O emissions during the growing season over the vetch crops but, in this study, did not. In fact, none of the CCs were effective in reducing N_2O emissions compared to fallow plots. The wheat and vetch results agree with a similar study of the fate of N under legume and non-legume overwintered CCs in Scotland (Baggs et al., 2000), but contradicts the results of nine studies compiled in a meta-analysis by Han et al. (2017). Han et al. (2017) calculated a 58% reduction of N_2O emissions on average from CCs during the growing phase. A wet spring (20 centimeters total rainfall in April and May versus 16 centimeters normally) may have suppressed plant growth (and thus the demand for N) and reduced the CC effect. At the time of plant incorporation in mid-June, plant biomass was less than the target amount considered necessary to realize the environmental and economic benefits of CCs.

It is possible that the N demand was not significantly different between CC types. One proxy for N demand, plant C:N ratio, did not correlate with N_2O fluxes or leaching during the growing period (data not shown). This is in contrast with a study of CC mixtures where the plant C:N ratio was positively related to a reduction in NO_3 leaching (Finney et al., 2016).

Fertilizer application to a CC is an uncommon practice when CCs are utilized for N conservation. However, to gain an understanding of the N_2O emissions of plots under higher soil N conditions, we applied an amount of fertilizer recommended to establish winter wheat. The fertilized plots produced greater N_2O emissions, but

only during the growing period. Post-tillage, the effect of the fertilizer was not detectable, indicating that the added N was either taken up by the plant or lost through denitrification or leaching before tillage. By comparison, an application of swine manure to a rye CC at similar N rates (179-195 kg-N ha^{-1} versus 224 kg-N ha^{-1} in this experiment) produced significantly more N_2O emissions and NO_3 leaching than its unfertilized CC treatments (Parkin et al., 2006).

Nitrate Leaching Losses in the Growth Period

The decrease in NO_3 leaching under wheat, vetch, and CC mixtures relative to fallow plots is consistent with the findings of studies in similar climates (McCraken et al., 1994, Meisinger and Ricigliano, 2017), although the effectiveness of overwintered CCs in reducing N leaching is variable and sensitive to local hydrologic conditions like weather and soil type, as well as CC planting date (Teixeira et al., 2016). With a wetter than average spring, we observed significant reductions in NO_3 leaching under our CC plots (Figure 7).

Results from the soil columns and resin bead capture system should be considered relative NO_3 losses among several CC types and not indicative of true leaching fluxes. Core installation could induce short-term decomposition of severed roots and hyphae or restricted root growth, both which may impact N cycling. In this experiment, core installation took place when the plants were small and root disturbance was unlikely to disproportionately affect one plant type over another. By restricting the horizontal space for root growth, the soil columns may also have forced plants to develop an uncharacteristic root biomass density. Root biomass density and rooting depth are negatively correlated with the amount of inorganic N leaching (Thorup-Kristensen, 2001). Anecdotally, we did not observe restricted

root growth in the columns, but this is a limitation that should be considered with this method. Other researchers using different methods of leachate collection showed similar results, indicating that the findings from this method were not wholly artifacts of the chosen methods.

Nitrous Oxide Losses in the Post-Tillage Period

Higher N_2O emissions in vetch plots during the post-tillage period can be explained by greater availability of N and higher soil temperatures. The Basche et al. (2014) meta-analysis found N_2O emissions increased under legume residues in 12 out of 15 observations compared to fallow fields. In contrast, Guardia et al. (2016) and Sanz-Cobena et al. (2014) found non-legume CCs emitted greater N_2O than legume CCs after the crops were killed and incorporated, though their measurement period was longer than in our study. Both studies measured for about 4 months following incorporation.

Soil microbes decomposing high C:N residue immobilize more soil N than material with a low C:N ratio (Baggs et al., 2000). From a mass balance perspective, greater soil N immobilization decreases the potential for N_2O production. In our study, the plant C:N ratio correlated negatively with N_2O in the post-tillage period, although this trend was heavily influenced by the few wheat plots at the higher end of C:N ratios. Our findings match the non-significant results of Han et al.'s meta-analysis (2017) comparing N_2O emissions and cover crop C:N ratio, suggesting the C:N ratio of CC plant matter impacts the cumulative N_2O emissions. Thus, we agree with Rayns and Lennartson's (1995) suggestion to plant cash crops a month after incorporation of high C:N CC residue and much sooner for lower C:N residue. Doing so ensures the greatest N uptake by plants and

minimizes the N losses a farmer might seek to avoid by planting a CC.

In another measure of N availability, we propose an alternative explanation for the difference of N_2O emissions in vetch and wheat residues. A positive relationship between N_2O emissions post-tillage and total plant N under vetch and negative one under wheat suggests that the wheat had not yet reached a sufficient degree of decomposition to stimulate additional N_2O production. Instead, lower N_2O emissions in wheat plots with a higher plant N indicates greater temporary sequestration of N from the soil via plant uptake. Wheat and mixture plots accumulated more N into plant tissues during the growing period, such that when these plots were tilled, sparking a release of C, there was less soil N available to microbes for N_2O production than in the vetch and fallow plots. Short-term N_2O release post-tillage has been shown to be greater under legumes than non-legume crops (Rosecrance et al., 2000) and we confirmed this in our experiment. Future work that closely tracks CC residue decomposition and soil N immobilization rates could illuminate the importance of each mechanism in N2O emissions from CC incorporation.

Conclusion

Growing concern for understanding the environmental impact of human activities such as row crop agriculture is driving the need for more research into CCs' ability to reduce N_2O emissions and NO_3 leaching losses. By studying both leaching and N_2O losses, we can understand how CCs might be used to improve N conservation in agricultural systems.

This study demonstrated that the environmental benefits of CCs depend on the type

and period of analysis. Legume CCs increased N_2O emissions to the atmosphere post-tillage over our non-legume CCs. Neither legume nor non-legume, nor a mixture of the two, was effective at reducing N_2O during the growth phase relative to fallow conditions. In addition, indirect N_2O emissions from denitrification of leached NO_3 may add to the climate benefit of non-legume CCs. Leaching measurements in the post-tillage period are recommended to assess the wider picture of avoided N_2O emissions through reduced leaching.

LITERATURE CITED

Anthony, W. H., Hutchinson, G. L., & Livingston, G. P. (1995). Chamber Measurement of Soil-Atmosphere Gas Exchange: Linear vs. Diffusion-Based Flux Models. *Soil Science Society of America Journal*, *59*(5), 1308. http://doi.org/10.2136/sssaj1995.03615995005900050015x

Baggs, E. M., Watson, C. A., & Rees, R. M. (2000). The fate of nitrogen from incorporated cover crop and green manure residues. *Nutrient Cycling in Agroecosystems*, *56*(2), 153–163. http://doi.org/10.1023/A:1009825606341

Basche, A. D., Miguez, F. E., Kaspar, T. C., & Castellano, M. J. (2014). Do cover crops increase or decrease nitrous oxide emissions? A meta-analysis. *Journal of Soil and Water Conservation*, *69*(6), 471–482. http://doi.org/10.2489/jswc.69.6.471

Bower, C.E., Holm-Hansen, T. (1980). A Salicylate–Hypochlorite Method for Determining Ammonia in Seawater. *Canadian Journal of Fisheries Aquatic Sci*ences 37, 794–798.

Christianson, L. E., & Harmel, R. D. (2015). 4R Water Quality Impacts: An Assessment and Synthesis of Forty Years of Drainage Nitrogen Losses. *Journal of Environment Quality*, *44*(6), 1852. http://doi.org/10.2134/jeq2015.03.0170

Erisman, J. W., Galloway, J. N., Seitzinger, S., Bleeker, A., Dise, N. B., Petrescu, A. M. R., … de Vries, W. (2013). Consequences of human modification of the global nitrogen cycle. *Philosophical Transactions of the Royal Society of London. Series B, Biological Sciences*, *368*(1621), 20130116. http://doi.org/10.1098/rstb.2013.0116

Finney, D. M., White, C. M., & Kaye, J. P. (2016). Biomass Production and Carbon/Nitrogen Ratio Influence Ecosystem Services from Cover Crop Mixtures. *Agronomy Journal*, *108*(1), 39. http://doi.org/10.2134/agronj15.0182

Guardia, G., Abalos, D., García-Marco, S., Quemada, M., Alonso-Ayuso, M., Cárdenas, L. M., … Vallejo, A. (2016). Effect of cover crops on greenhouse gas emissions in an irrigated field under integrated soil fertility management. *Biogeosciences*, *13*(18), 5245–5257. http://doi.org/10.5194/bg-13-5245-2016

Han, Z., Walter, M. T., & Drinkwater, L. E. (2017). N2O emissions from grain cropping systems: a meta-analysis of the impacts of fertilizer-based and ecologically-based nutrient management strategies. *Nutrient Cycling in Agroecosystems*, *107*(3), 335–355. http://doi.org/10.1007/s10705-017-9836-z

Hardarson, G., & Atkins, C. (2003). Optimising biological N ₂ fixation by legumes in farming systems. *Plant and Soil*, *252*(1), 41–54. http://doi.org/10.1023/A:1024103818971

Hutchinson, G., & Mosier, A. (1981). Improved Soil Cover Method for Field Measurement of Nitrous Oxide Fluxes. *Soil Science Society of America Journal*, *45*, 311–316.

Kjønaas, O. J. (1999). Factors Affecting Stability and Efficiency of Ion Exchange Resins in Studies of Soil Nitrogen Transformation. *Communications in Soil Science and Plant Analysis*, *30*(January 2015), 2377–2397. http://doi.org/10.1080/00103629909370380

Kjønaas, O. J. (1999). In Situ Efficiency of Ion Exchange Resins in Studies of Nitrogen Transformation. *Soil Science Society of America Journal*, *63*, 399. http://doi.org/10.2136/sssaj1999.03615995006300020019x

McCracken, D. V., Smith, M. S., Grove, J. H., Blevins, R. L., & MacKown, C. T. (1994). Nitrate Leaching as Influenced by Cover Cropping and Nitrogen Source. *Soil Science Society of America Journal*, *58*(5), 1476. http://doi.org/10.2136/sssaj1994.03615995005800050029x

Meisinger, J. J., Hargrove, W. L., Mikkelsen, R. L., Williams, J. R., & Benson, V. W. (1991). Effects of cover crops on groundwater quality. *Cover Crops for Clean Water. Soil and Water Conservation Society*, (c), 57–68.

Meisinger, J. J., & Ricigliano, K. A. (2017). Nitrate Leaching from Winter Cereal Cover Crops Using Undisturbed Soil-Column Lysimeters. *Journal of Environment Quality*, *0*(0), 0. http://doi.org/10.2134/jeq2016.09.0372

Northeast Regional Climate Center (2018). http://climod2.nrcc.cornell.edu. Accessed 17 November 2018.

O'Dell, J.W. (1993). Determination of nitrate-nitrite nitrogen by automated colorimetry. Method 353.2.

Parkin, T. B., Kaspar, T. C., & Singer, J. W. (2006). Cover crop effects on the fate of N following soil application of swine manure. *Plant and Soil*, *289*(1–2), 141–152. http://doi.org/10.1007/s11104-006-9114-3

Parkin, T. B., & Venterea, R. T. (2010). Sampling Protocols. Chapter 3. Chamber-Based Trace Gas Flux Measurements. In R. Follett (Ed.), *Sampling Protocols* (Vol. 2010, pp. 3-1-39). Retrieved from www.ars.usda.gov/research/GRACEnet

Ranells, N. N., & Wagger, M. G. (1996). Nitrogen release from grass and legume cover crop monocultures and bicultures. *Agronomy Journal*, *88*(5), 777–782. http://doi.org/10.2134/agronj1996.00021962008800050015x

Rayns, F. W., & Lennartsson, E. K. M. (1995). The nitrogen dynamics of winter green manures. In H. Cook & H. Lee (Eds.), *Soil Management in Sustainable Agriculture* (pp. 308–311). Wye College Press.

Reiss, E. (2018). *Impact of plant community diversity on agriculturally important ecosystem services in cash and cover crop systems*. Cornell University.

Rosecrance, R. C., Mccarty, G. W., Shelton, D. R., & Teasdale, J. R. (2000). Denitrification and N mineralization from hairy vetch (Vicia villosa Roth) and rye (Secale cereale L.) cover crop monocultures and bicultures. *Plant and Soil*, *227*(1–2), 283–290. http://doi.org/10.1023/A:1026582012290

Sainju, U. M., Stevens, W. B., Caesar-Tonthat, T., & Liebig, M. A. (2012). Soil greenhouse gas emissions affected by irrigation, tillage, crop rotation, and nitrogen fertilization. *Journal of Environmental Quality*, *41*(6), 1774–86. http://doi.org/10.2134/jeq2012.0176

Sanz-Cobena, A., García-Marco, S., Quemada, M., Gabriel, J. L., Almendros, P., & Vallejo, A. (2014). Do cover crops enhance N2O, CO2 or CH4 emissions from soil in Mediterranean arable systems? *Science of The Total Environment*, *466–467*, 164–174. http://doi.org/10.1016/j.scitotenv.2013.07.023

Sebestyen, S. D., Boyer, E. W., Shanley, J. B., Kendall, C., Doctor, D. H., Aiken, G. R., & Ohte, N. (2008). Sources, transformations, and hydrological processes that control stream nitrate and dissolved organic matter concentrations during snowmelt in an upland forest. *Water Resources Research*, *44*(12), 1–14. http://doi.org/10.1029/2008WR006983

Shearer, G., & Kohl, D. (1986). N 2 -Fixation in Field Settings: Estimations Based on Natural 15 N Abundance. *Australian Journal of Plant Physiology*, *13*(6), 699. http://doi.org/10.1071/PP9860699

Teixeira, E. I., Johnstone, P., Chakwizira, E., de Ruiter, J., Malcolm, B., Shaw, N., … Curtin, D. (2016). Sources of variability in the effectiveness of winter cover crops for mitigating N leaching. *Agriculture, Ecosystems and Environment*, *220*, 226–235. http://doi.org/10.1016/j.agee.2016.01.019

Thorup-Kristensen, K. (2001). Are differences in root growth of nitrogen catch crops important for their ability to reduce soil nitrate-N content, and how can this be measured? *Plant and Soil*, *230*(2), 185–195.

Tonitto, C., David, M. B., & Drinkwater, L. E. (2006). Replacing bare fallows with cover crops in fertilizer-intensive cropping systems: A meta-analysis of crop yield and N dynamics. *Agriculture, Ecosystems & Environment*, *112*(1), 58–72. http://doi.org/10.1016/j.agee.2005.07.003

Van Bochove, E., Jones, H. G., Pelletier, F., & Prevost, D. (1996). Emission of N2O from agricultural soil under snow cover: A significant part of N budget. *Hydrological Processes*, *10*(11), 1545–1549. http://doi.org/10.1002/(SICI)1099-1085(199611)10:11<1545::AID-HYP492>3.0.CO;2-0

Wagger, M. G., Cabrera, M. L., & Ranells, N. N. (1998). Nitrogen and carbon cycling in relation to cover crop residue quality. *Journal of Soil and Water Conservation*, *53*(3), 214–218. Retrieved from http://www.jswconline.org/content/53/3/214.short

Wagner-Riddle, C., Thurtell, G. W., Kidd, G. K., Beauchamp, E. G., & Sweetman, R. (1997). Estimates of nitrous oxide emissions from agricultural fields over 28 months. *Canadian Journal of Soil Science*, *77*(2), 135–144. http://doi.org/10.4141/S96-103

Wagner-Riddle, C., Congreves, K. A., Abalos, D., Berg, A. A., Brown, S. E., Ambadan, J. T., … Tenuta, M. (2017). Globally important nitrous oxide emissions from croplands induced by freeze–thaw cycles. *Nature Geoscience*, *10*(4), 279–283. http://doi.org/10.1038/ngeo2907

World Meterological Organization. (2016). *WMO Greenhouse Gas Bulletin: The State of Greenhouse Gases in the Atmosphere Based on Global Observations*

through 2015.

CHAPTER 2
GRID SCALE COMPARISON OF NITROGEN CYCLING IN THE COMMUNITY LAND MODEL

Introduction

Coupled ocean, land, and atmospheric models are used to explore outcomes of a changing global climate and estimate the impact of human activities (e.g. IPCC, 2014). Earth Surface Models (ESMs) have been developed to account for feedbacks occurring between the Earth's general circulation and biogeochemical cycles (Gruber & Galloway, 2008, Arneth et al., 2010). Accurate representation of the carbon cycle and sequestration on land has immediate relevance for understanding future CO_2 levels and climate responses. The incorporation of the nitrogen (N) cycle in ESMs attempts allows simulation of this regulator of the carbon cycle through its effects on microbial decomposition and plant growth (e.g., Bonan and Levis, 2010, Lawrence et al., 2011). The addition of an N cycle also provides a direct estimate of nitrous oxide (N_2O), an important and long-lived greenhouse gas (Prather et al., 1995). N_2O is primarily produced by the microbially-mediated processes of nitrification and denitrification (Butterbach-Bahl, et al., 2013). ESMs that include a nitrogen cycle demonstrate a smaller CO_2 fertilization effect and less temperature sensitivity than carbon-only models (Arora et al., 2013). While the addition of N to global land surface models was heralded as a promising direction in Earth System Modeling (Friedlingstein et al., 2006), there has been much concern about the accuracy of coupled C-N cycling in Earth System Models (Zaehle and Dalmonech, 2011; Thomas et al. 2013), and more specifically, in simulating the critical N loss process of denitrification in the Community Land Model (CLM) (Houlton et al., 2015).

The progress of Land Surface Models (LSMs) in providing provide energy, water, and biogeochemical boundary conditions for the general circulation in ESMs led to their development at spatial scales primarily optimized for the computation of global energy fluxes and regional atmospheric and ocean circulation [i.e. the general circulation]. By contrast, water flux and storage in the vadose zone are often described by the hydrologic community as a plot-scale state variable with large spatial heterogeneity across the catchment scale (e.g. Buchanan et al., 2014). LSMs, however, commonly resolve soil moisture transport at a fine vertical resolution (e.g. 1 m soil layers) via a physically-based model (e.g. Richards Equation) (Clark et al., 2015b), while averaging horizontal heterogeneity to a very coarse resolution (e.g. 1 degree).

Issues of scale have long been recognized as a challenge in developing a universal water flux framework (Fatichi et al., 2016; Blöschl & Sivapalan, 1995). Ideally, a model's spatial resolution should have little effect on how state variables are resolved. Disparity between the spatial and temporal scales at which hydrologic and biogeochemical processes can be measured, simulated, and the scales at which these processes actually occur, introduces uncertainty in our understanding of and ability to reproduce them (Kirchner, 2006). Physically-based water fluxes in hydrologic and biogeochemical models are commonly averaged across spatial heterogeneity (e.g. soil moisture, groundwater elevation, plant water uptake) via scale-dependent parameterizations of water fluxes (Beven et al., 2014), potentially limiting the physical meaning and relevance of cross-scale model linkages (Clark et al., 2015a, b).

Recent research has highlighted process-based issues in land surface hydrologic models related to "upscaling" plot- and hillslope-scale processes to the coarse

regional resolutions demanded by ESMs. Shrestha et al. (2015) evaluated the sensitivity of shallow soil moisture and surface energy flux to model grid resolution in the TerrSysMP, where model predictions of both soil moisture and energy flux were highly dependent on grid scale. Nijzink et al. (2016) demonstrated the importance of maintaining hydrologically relevant topographic features in a distributed regional hydrologic model. Resolutions that overly-smoothed relevant features resulted in a loss of hydrologic model calibration performance in simulating surface water discharge. Freund & Kirchner (2017) demonstrated that under-representation of spatial heterogeneity in a LSM may overestimate evapotranspiration (ET), and underestimate soil moisture. Numerical grids treat the vadose zone as spatially averaged columns of soil moisture that conserve mass at the grid scale. Decreasing model resolution implicitly incorporated an assumption of high lateral soil moisture transfer potential, a process which may violate our understanding of the sub-grid mass balance (Freund & Kirchner 2017). Tesfa et al. (2016) demonstrated surface runoff sensitivity to model grid scales of 1/4º, 1/2º, and 1º where total annual runoff was higher in coarser resolutions of the model. Conversely, Shrestha et al. (2018) found that coarser resolutions of the CLM produced higher soil water contents. The complexity of the hydrologic cycle and grid-scale dependency is illustrated by the contrasting results of Freund& Kirchner (2017), Tesfa et al. (2016), and Shrestha et al. (2015; 2018). Sensitivity of physical and biological processes to grid scale can modulate competing catchment outflow pathways of ET and discharge in unexpected ways. It is therefore likely that hydrologic uncertainty related to the degree of spatially averaging depends on location, model formulation and parameterization, and grid scale. In addition, this averaging approach could yield inaccurate predictions of biogeochemical processes such as denitrification that depend on threshold or other nonlinear responses to moisture conditions,

temperature, and other environmental drivers.

Soil N biogeochemical processes are particularly challenging to incorporate into regional LSMs given the extreme spatial and temporal variability at which many of these processes occur (Groffman et al., 2009). Challenges in developing reliable numerical models of nitrification and denitrification are underscored by the continuing difficulty in developing a community-accepted conceptual model to describe heterogeneous hot spot and hot moment behavior (Bernhardt et al., 2017). Further, nitrification and denitrification often depend on the hydrologic cycle and its role in supplying substrates for these microbial processes and in affecting oxygen levels. That is, during nitrification, autotrophic bacteria require oxygen for the conversion of ammonium to nitrate, while during denitrification, heterotrophic microbes use nitrate as an electron acceptor to consume organic matter when oxygen is scarce. Soil water levels create anaerobic soil conditions, while surface runoff and subsurface drainage transport the necessary substrates (e.g. ammonium, nitrate (NO_3), and dissolved organic carbon). At the catchment scale, heterogeneity of soil and groundwater describes the spatial patterns in runoff generation and dissolved N losses (e.g. Knighton et al., 2017). We anticipate that scale-dependent issues in the hydrologic cycles of LSMs, described above, will propagate and magnify uncertainty in the N cycle. In response to these challenges, attempts to upscale soil N biogeochemical processes such as denitrification to ESM resolutions have typically relied on empirical relationships between nutrient availability and environmental conditions (Boyer et al., 2006). Column-, plot-, and hill-slope scale denitrification experiments all carry implicit assumptions about the scale-relevance of the relationships they define (e.g. Parton et al., 1988), which deserve some consideration when incorporated into a regional model.

Here, we examined the scale-dependency of several N cycle processes in the CLM4.5 (Lawrence et al., 2011, Koven et al. 2013), a model with previously identified scale issues in its hydrologic cycle (e.g. Tesfa et al., 2016; Shrestha et al., 2018), and recognized difficulty in simulating gaseous and hydrologic-driven N losses (Koven et al., 2013, Houlton et al. 2015). Our research questions are as follows:

Is the CLM4.5 prediction of the soil N processes nitrification, denitrification, and nitrate leaching grid scale-dependent?

Can any observed discrepancies in these soil N processes across grid-scales be explained by issues in hydrologic scale-dependence, by biogeochemical processes, or other factors?

Methods

Model Description

CLM4.5 (Koven et al. 2013) discretizes the land surface into regular grid cells, each with a 15-layered soil column with increasingly thicker layers (0.0175 m < Δz 13.85 m). The soil hydrologic and biogeochemical column has a maximum depth of 3.8 m, whereas the soil temperature column extends to 48 m. The grid cell is summarized as a surface with several plant functional types (PFTs) that draw nutrients from the same shared soil pool. In CLM4.5, plants access all layers in the soil column to their rooting depth as determined by the plant water uptake model. We ran the model with the default 30-minute time-step and gathered outputs into monthly averages.

The model is forced with precipitation data aggregated to the spatial resolution of the LSM. Surface and subsurface water flows are simulated using a simplified TOPMODEL approach (Oleson et al., 2008). Hydrologic flows are unidirectional

inputs to a separate river routing model.

The soil biogeochemistry in CLM4.5 (and in the recently released CLM5.0) consists of a coupled carbon and N cycle based on the Century model (Parton et al., 1988; see Koven, et al., 2013). Mineral N is subdivided into ammonium (NH_4) and NO_3 pools. Mineralization of N from soil organic matter and leaf litter contribute to the NH_4 pools. Plants and soil microbial immobilizers take up N from both inorganic N pools, while nitrifiers consume only NH_4 and denitrifiers only NO_3. N demand from nitrifiers and denitrifers is a function of their substrate availability, scaled by the aerobic (nitrification) or anaerobic (denitrification) fraction in the soil layer. This fractional partitioning is calculated using a mechanistic model developed from laboratory column experiments and is intended to simulate anoxic micro-sites in heterogeneous soil matrices (Arah & Vinten, 1995). The NO_3 that remains at the end of each timestep is available to runoff and leaching. The flux of NO_3 exported in this manner is determined by the NO_3 concentration in the soil layer and the volume of surface or subsurface flow.

Experimental Design

We tested the scalability of the N cycle in CLM4.5 for the region surrounding the Hubbard Brook Experimental Forest (HBEF) (43.933926, -71.735448), in the White Mountains of New Hampshire, USA. We selected this watershed because it has significant topographic variation as well as long-term records of streamflow and hydrologic N losses. Steeper terrain should produce more soil moisture heterogeneity, and create difficulty in modeling soil moisture with CLM. The HBEF (43.933926, -71.735448) has steep slopes and well-draining, acidic Spodosols (Soil Survey Staff, 2006). Its vegetation is largely broadleaf deciduous forest, typical of the Northeastern US, dominated by *Fagus grandifolia* (American

beech), *Acer saccharum* (sugar maple), and *Betula alleghaniensis* (yellow birch), with the needleleaf evergreens red spruce *(Picea rubens)* and balsam fir *(Abies balsamea)* at higher elevations (Schwartz et al., 2003). The HBEF has a cool temperate, humid continental climate. Annual precipitation is 1400 mm with almost 1/3 delivered as snow (Likens et al., 2013). The ground is typically snow-covered from late December to mid-April (Morse et al., 2015).

We used the offline, point mode of CLM4.5 and a 110-year (1901-2010) atmospheric forcing dataset (CRUCEP; Viovy, 2011). Using the extraction tools available through CLM development group, we created three land surface datasets of the ~9000 km^2 region with resolutions of 1.0°, 0.5°, and 0.3°. The total region of analysis was approximately the same for each resolution (max difference of 0.1 km^2), but the number and area of grid cells differed (Table 1).

Table 1 CLM4.5 Grid Cell Area Comparison

Model Resolution	**Number of Grid Cells**	**Average Grid Cell Size (km^2)**
0.3°	9	988
0.5°	4	2224
1.0°	1	8894

The PFTs automatically selected with the surface dataset creation tool were not altered. The proportion of each PFT was maintained for the entire region (72% broadleaf deciduous trees, 20% needleleaf evergreen trees, 3% agricultural crops, 2% broadleaf deciduous boreal trees, 1% needleleaf evergreen boreal trees, and <1% arctic grass), but the distribution of PFTs in each cell varied. The percent sand content and clay content in the surface datasets were changed to better match

ground-based HBEF observations. For simplicity, we assume that the soils are uniform percentages of clay (changed from 11-19 to 3%) and sand (changed from 45-64 to 71%). These soil texture values were also used in a previous analysis at HBEF using CLM4.5 (Wieder et al., 2015) and originated from soil data from Zak et al., (1994).

The model was spun up according to prescribed methods to steady state conditions. Each model resolution was spun up individually because of difficulty in aggregating initial conditions files to lower resolutions. The model was spun up for approximately 2200 simulation years until the annual change in soil N storage was less than 0.004%.

After spin up, the model was run with climate and N deposition data for the years 1991-2010. The forcing data is applied at the same resolution as the surface data. We compared the monthly average rates of focal N cycle processes for this 20-year period for each resolution aggregated to 1° and used a one-sample, nonparametric Wilcoxon test on the differences between resolutions.

To determine the sensitivity of several modeled N processes to state variables, we examined relationships between seasonal and annual rates of denitrification, nitrification, and leaching (the dependent variables) versus their likely state variables (the independent variables). Slopes were tested for significant differences from zero, and R^2 values were used to select the relationship that best explained the seasonal variation in the dependent variable. We interpret the R^2 value as an objective measure of sensitivity.

Results

There were significant differences in annual nitrification rates between all

resolutions, in that more coarsely resolved models consistently yielded lower annual nitrification rates than more finely resolved implementations (Table 2). For denitrification, the coarsest resolution (1°) produced significantly lower annual denitrification rates than the 0.3° and 0.5° simulations.

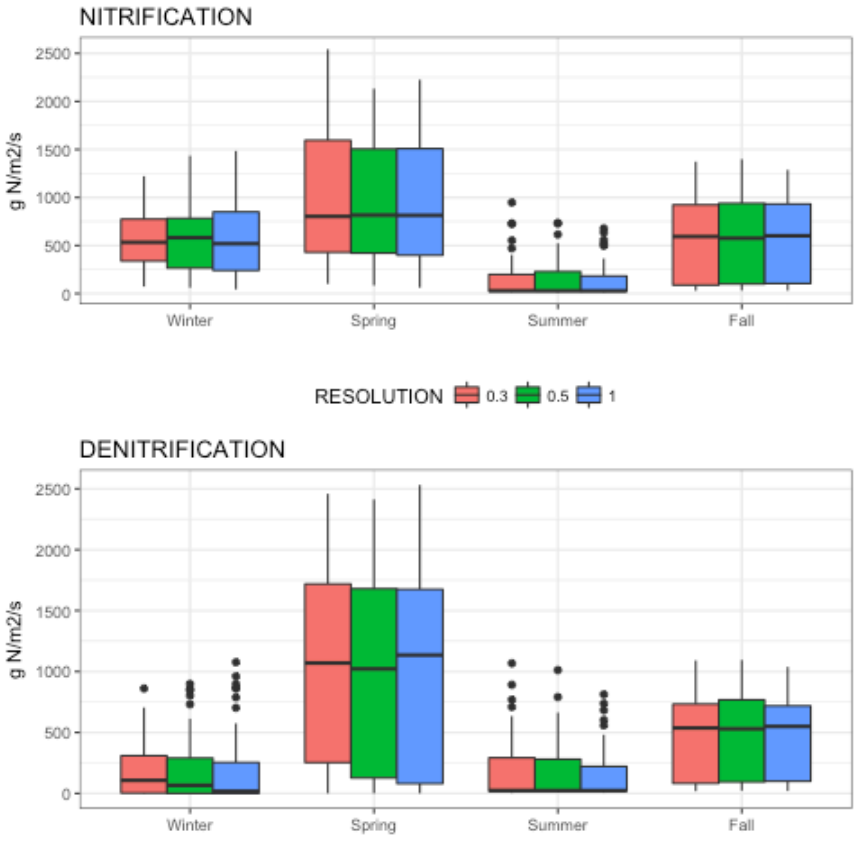

Figure 11 Scaling behavior of nitrification (top) and denitrification (bottom) in CLM4.5 for each 3-month season. Center lines show the medians. Box limits indicate the 25th and 75th percentiles, with whiskers extending 1.5 times the interquartile range. Outliers are represented by dots.

Table 2 Summary Statistics of the Annual Differences in Nitrification and Denitrification Rates Between Model Resolutions

	Nitrification Differences			**Denitrification Differences**		
Model Resolutions Compared	Mean gN m^{-2}	standard deviation gN m^{-2}	Wilcoxn test statistic & p-value	Mean gN m^{-2}	standard deviation gN m^{-2}	Wilcoxn test statistic & p-value
0.5º / 0.3º	-5.840	152.8	**W=11484 p<0.0005**	-1.281	127.1	W= 15297 p=0.5797
1.0º / 0.5º	-8.033	84.83	**W=11441 p<0.0005**	-6.192	115.9	**W=11148 p<0.0005**
1.0º / 0.3º	-13.87	168.9	**W=9486 p<0.0005**	-7.472	174.1	**W=11849 p<0.0005**

The differences in annual nitrification and denitrification rates between scales, however, were not consistent across seasons. In winter, differences between resolutions were small and non-significant (Table 3). In the summer, resolutions all differed significantly from one another ADD detail on what these differences were: direction and magnitude. . This result indicates that a scalability issue in one of the environmental variables driving nitrification and denitrification modules was responsible for the different values.

Table 3 Wilcoxon Test P-values for Seasonal Differences in Nitrification (NIT) and Denitrification (DN) Rates Between Scales

Model Resolutions Compared	**N Flux**	**Winter**	**Spring**	**Summer**	**Fall**
0.5º / 0.3º	NIT	0.707	<0.0005	0.0183	0.1223
	DN	0.155	0.639	0.921	0.281

1.0º / 0.5º	NIT	0.719	0.183	<0.0005	0.00335
	DN	0.0681	0.479	<0.0005	<0.0005
1.0º / 0.3º	NIT	0.591	<0.0005	<0.0005	0.000538
	DN	0.0212	0.217	0.00975	0.149

We used a simple linear regression-based sensitivity analysis to assess when various likely regulators of nitrification or denitrification (i.e., aerobic fraction, volumetric soil moisture, ammonium concentration, and soil temperature) were controlling these rates, and considered those factors a source of the scalability problem. The analysis revealed that monthly nitrification rate was most sensitive to soil temperature in the winter and spring (Figure 12, R^2=0.63 and R^2=0.88, respectively), and to soil NH_4 concentration in the summer and fall (R^2=0.98 and R^2=0.96, respectively). In winter and spring, high soil NH_4 availability supported nitrification, but temperature limited the microbial process. Once the soils warmed in the late spring, the soil NH_4 pool was quickly drawn down by nitrifiers and plants. As the soil NH_4 pool became depleted in summer, NH_4 availability limited nitrification until after the fall, when plants' demand decreased.

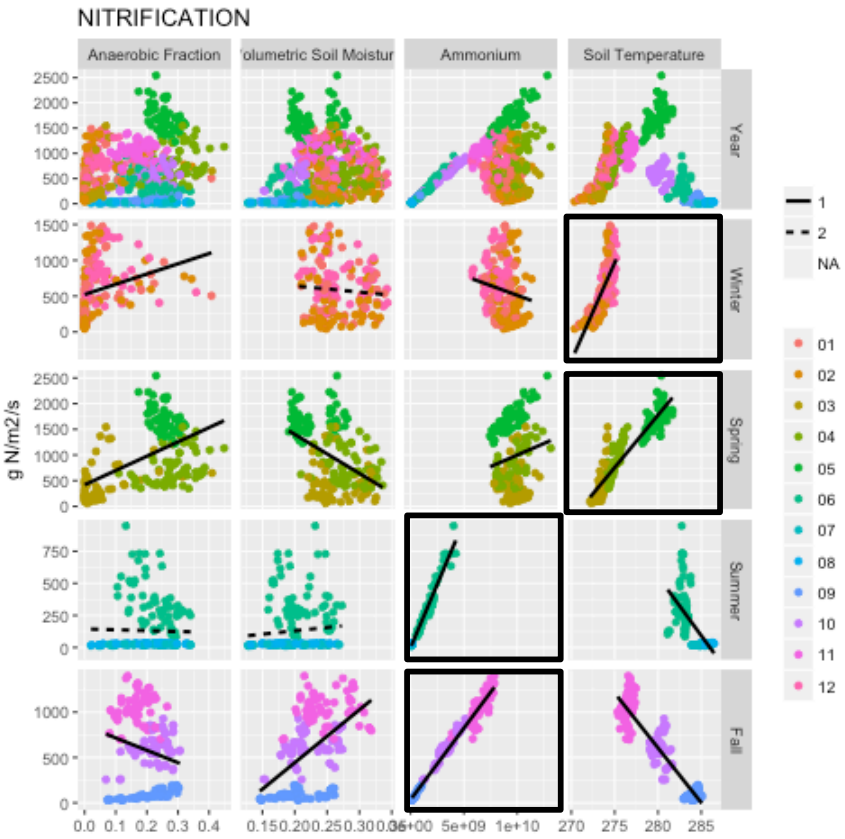

Figure 12 Monthly nitrification model rates were most sensitive to soil temperature in the winter and spring and to soil ammonium content in the summer and fall. Solid lines indicate a linear regression with a slope significantly different from zero. Boxed plots indicate linear regressions with the best fit as determined by coefficient of determination. Note the y-axes differ for each seasonal grouping.

Winter nitrification rates did not differ significantly across scales. In spring, differences in nitrification across model resolutions can be attributed in part, to scale-dependent differences in soil temperature differences. CLM produced higher soil temperature values at the finest resolution (Figure 13A), contributing to greater springtime nitrification on average. Secondarily, differences in soil moisture likely also contributed to the nitrification differences across scales (Figure 13B). The higher soil moisture at the finest resolution produced lower rates of nitrification,

partially counter-acting the scaling effect of temperature. Summer and fall nitrification rates were also different across the three scales, due to significant differences in the soil NH_4 concentrations (Figure 13C) and secondarily, due to differences in soil temperature. In summer and fall, significantly higher NH_4 concentrations in the middle resolution over the coarse grid increased the nitrification rate. Soil temperature was lowest in the fine resolution and differed significantly from the coarse grid, creating a difference in nitrification rates between these two resolutions. Note that the direction of the relationship between nitrification and soil temperature in the summer was the opposite of the winter and spring (Figure 12). That is, warmer soils negatively correlated with nitrification rates in winter and spring. In fall, nitrification rates were significantly lower in the coarse resolution compared to the fine and middle resolutions, despite the significantly higher NH_4 concentrations than the middle resolution model. Significantly lower NH_4 concentrations in the middle resolution explained the significantly lower nitrification rates of the middle compared to the fine resolution.

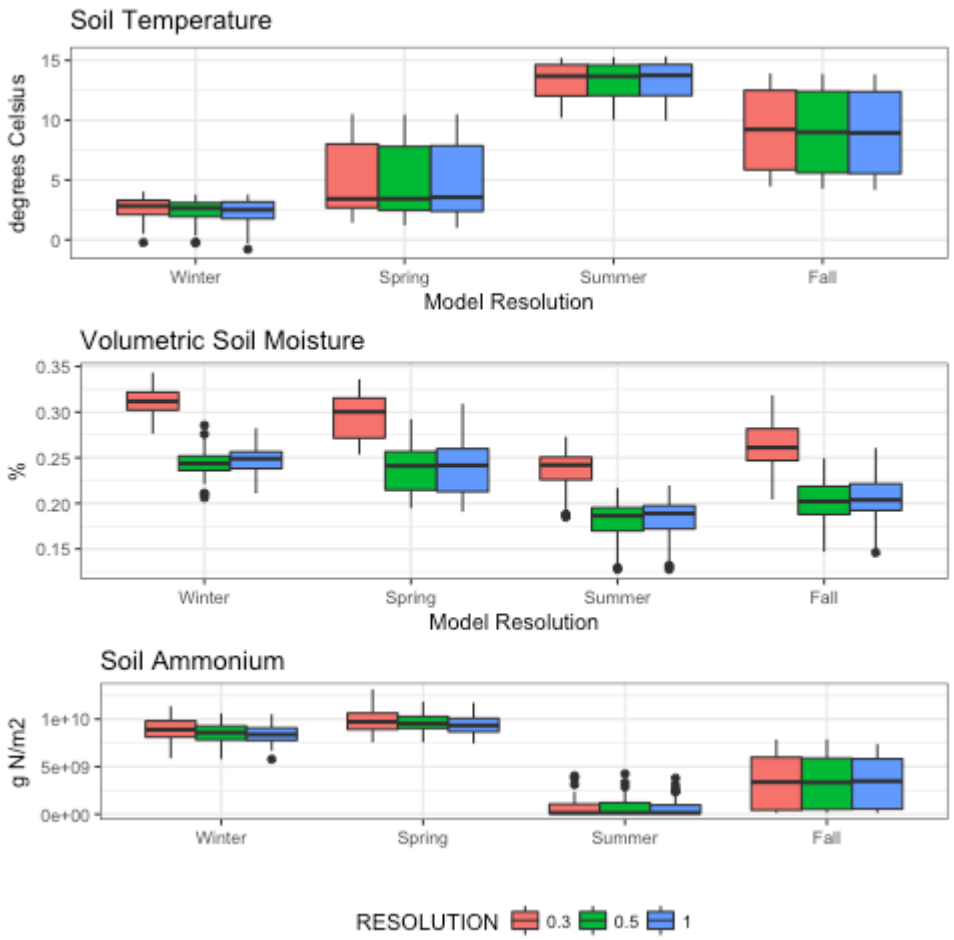

Figure 13 Scaling behavior of sensitive factors in nitrification. Soil temperature (top) controls nitrification in the winter and spring Soil moisture is a secondary control in the spring, while ammonium concentration determines summer and fall nitrification. Center lines show the medians. Box limits indicate the 25th and 75th percentiles, with whiskers extending 1.5 times the interquartile range. Outliers are represented by dots.

In the denitrification sensitivity analysis, monthly denitrification rates were generally more sensitive to substrate availability rather than to environmental factors (Figure 14). Heterotrophic respiration, which CLM4.5 uses as a proxy for carbon availability, correlated positively with denitrification rates in the winter and spring (R^2=0.75 and R^2=0.89 respectively), while the soil NO_3 concentration

correlated with monthly denitrification rates in summer and fall (R^2=0.91 and R^2=0.59 respectively). In winter and spring, NO_3 accumulated until soil temperatures rose above a threshold of about 2ºC, spurring both heterotrophic respiration and denitrification in late spring. Other microbial processes concerning the N cycle rapidly increased in late spring as well, including immobilization and nitrification (Figure 11). Plant uptake increased marginally in spring and steeply in the first month of summer. This plant uptake caused the soil NO_3 pool to drop and remain small until late fall after plant uptake ceased. Denitrification fell in the summer in response to low soil NO_3 availability which continued into fall. It increased again at the end of fall when plants no longer dominated uptake of the soil NO_3. Denitrification and its N substrate NO_3 followed the same seasonal trends as nitrification and NH_4.

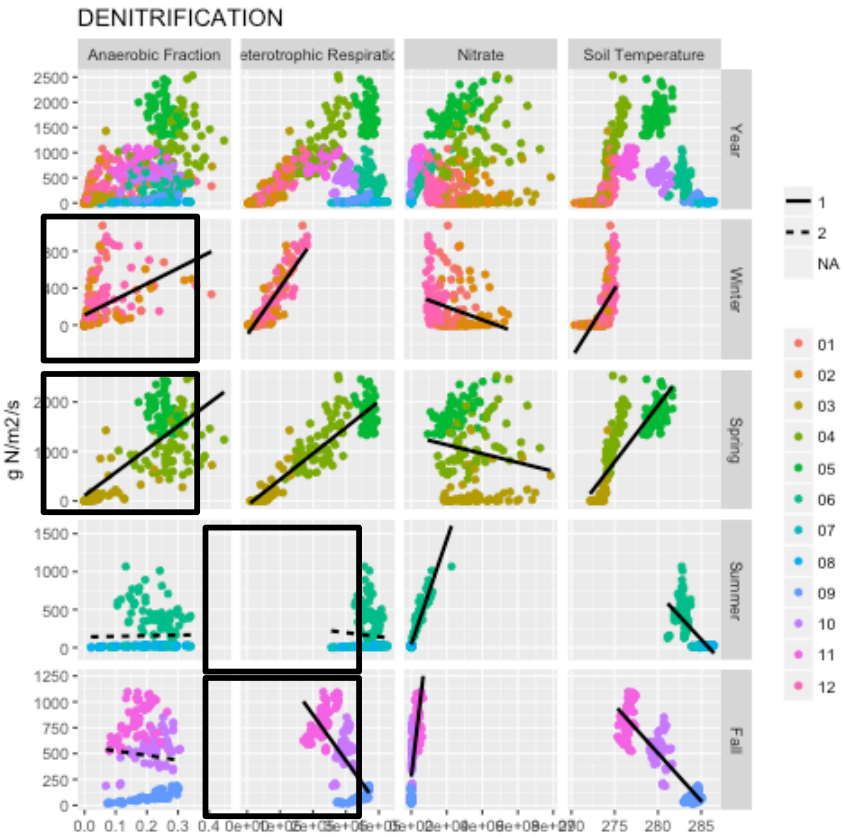

Figure 14 Monthly denitrification rate was most sensitive to heterotrophic respiration in the winter and spring and to soil nitrate concentration in the summer and fall. Solid lines indicate a linear regression with a slope significantly different from zero. Boxed panels indicate linear regressions with the best fit as determined by coefficient of determination. Note the y-axes differ for each seasonal grouping.

Winter differences in denitrification rates across the scales correlated most strongly with increases in heterotrophic respiration, and secondarily with increases in anaerobic fraction (Figure 15). With both of these drivers of denitrification, the finer resolution was significantly higher/lower than the middle and coarse resolutions. Greater heterotrophic respiration and a larger anaerobic soil fraction drove increased denitrification rates in the middle resolution. There were no differences in denitrification rates across scales in the spring months, despite some differences in heterotrophic respiration and soil temperate. Anaerobic fraction and

NO_3 conditions were similar across scales and may have countered the differences in heterotrophic respiration. Summer differences in denitrification rates can be attributed to differences in soil temperature and anaerobic fraction. That is, mean summer temperature and anaerobic fraction increased from fine to coarse resolution, and corresponded with increasing mean denitrification rates across these scales. By fall, of the combination of lower temperatures and NO_3 concentrations in the coarse resolution gave rise to significantly lower denitrification rates compared to the mid resolution simulations.

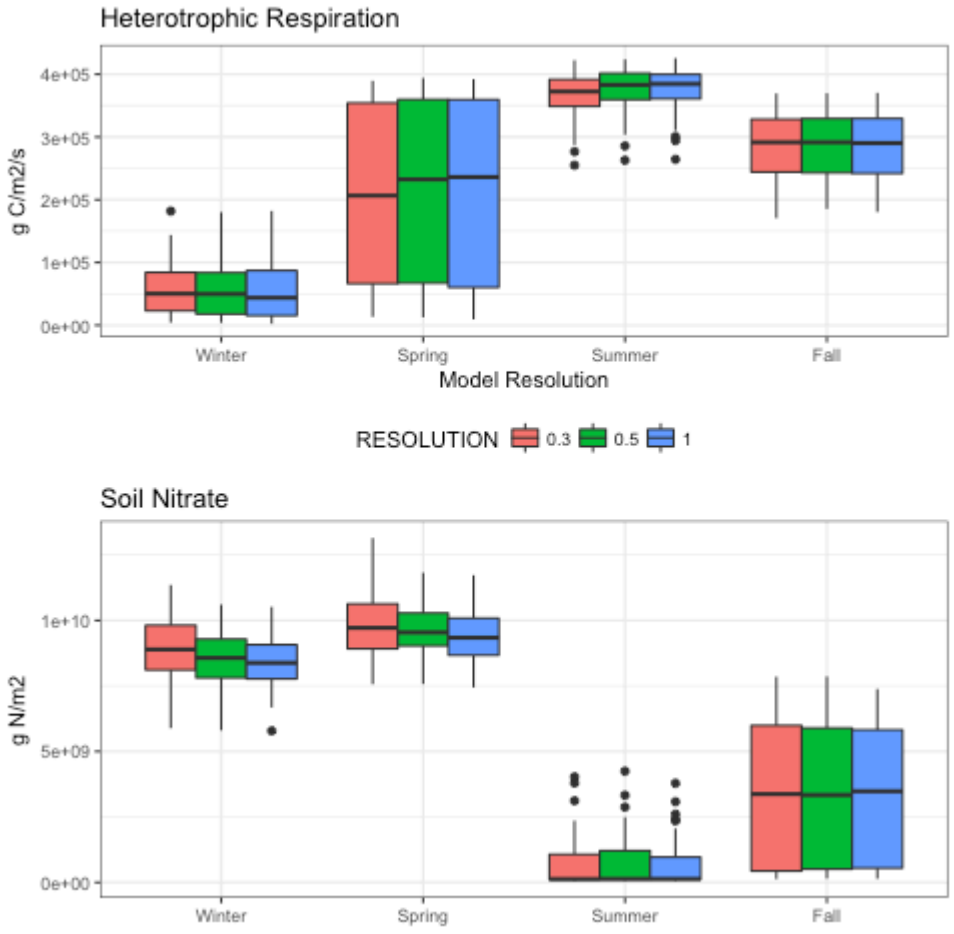

Figure 15 Scaling behavior of sensitive factors in denitrification. Heterotrophic respiration (top) controls denitrification in the winter and spring, while nitrate concentration determines summer and fall denitrification. Center lines show the

medians. Box limits indicate the 25th and 75th percentiles, with whiskers extending 1.5 times the interquartile range. Outliers are represented by dots.

Nitrate leaching differed across scales appeared in every season, in that the fine resolution simulations had less nitrate leaching the simulations at the middle or coarse scales (Figure 16). The middle and fine resolutions were consistently different across the year (Table 4). Leaching peaked in early spring, a month before the microbial processes that consume and immobilize NO_3 were activated and three months before plants reached peak uptake. Leaching is the final pathway for mobile soil N, thus the flux of N lost was many times smaller than other demands on the soil NO_3 pool. The sensitivity analysis demonstrated a sensitivity to the amount of subsurface drainage in the winter and spring (Figure 17, R^2=0.34 and R^2=0.88) and to soil NO_3 concentration in the summer and fall (R^2=0.73 and R^2=0.76). Subsurface drainage was significantly lower in the finest resolution in every season and likely drove the differences in leaching in winter and spring (Figure 18). Soil NO_3 concentration was lowest in the coarse resolution simulations. Under the comparatively low soil NO_3 conditions of the summer and fall, this scaling difference carried through as a significantly lower leaching mass in the coarse resolution.

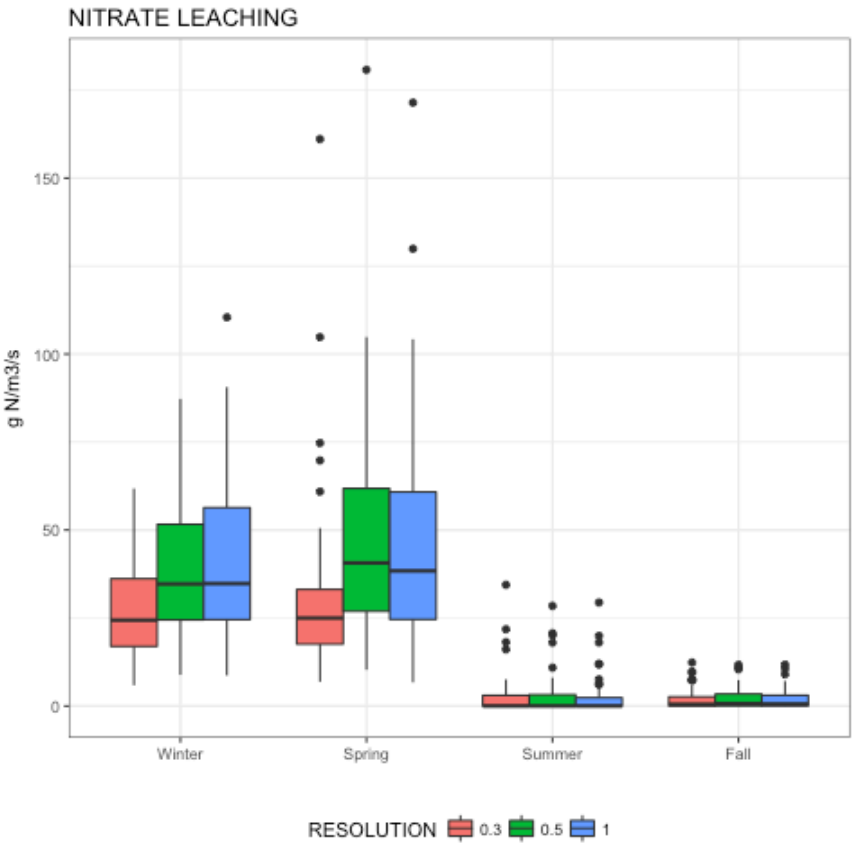

Figure 16 Scaling behavior of nitrate leaching through the seasons. Center lines show the medians. Box limits indicate the 25th and 75th percentiles, with whiskers extending 1.5 times the interquartile range. Outliers are represented by dots.

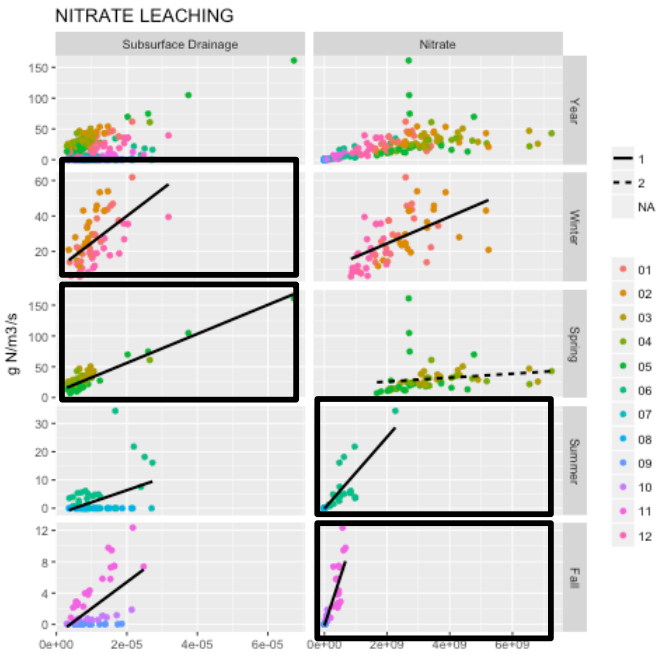

Figure 17 Nitrate leaching is sensitive to subsurface drainage in the winter and spring and soil nitrate content in the summer and fall. Data shown are from model simulations at 0.3 degree resolution. Solid lines indicate a linear regression with a slope significantly different from zero. Boxed plots indicate linear regressions with the best fit as determined by coefficient of determination. Note the y-axes differ for each seasonal grouping.

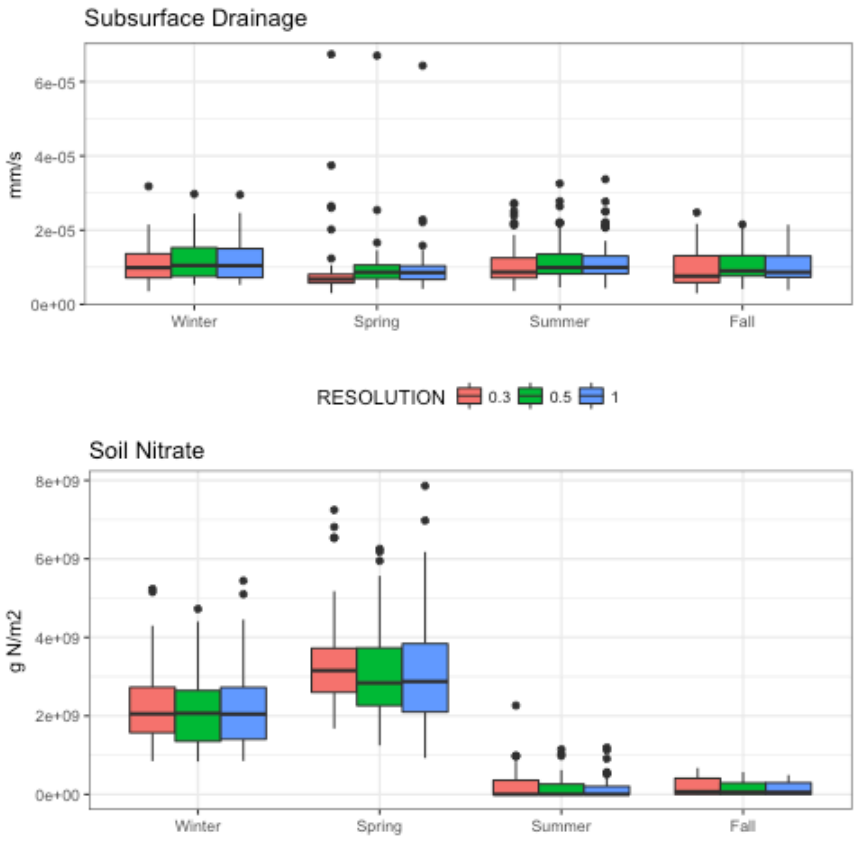

Figure 18 Scaling behavior of sensitive factors in nitrate leaching. Subsurface drainage (top) controls leaching in the winter and spring, while nitrate concentration determines summer and fall leaching. Center lines show the medians. Box limits indicate the 25th and 75th percentiles, with whiskers extending 1.5 times the interquartile range. Outliers are represented by dots.

Table 4 Wilcoxon Test P-values for Seasonal Differences in Leaching Rates Between Scales

Model Resolutions Compared	N Flux	Winter	Spring	Summer	Fall
0.5° / 0.3°	LEACH	**<0.0005**	**<0.0005**	**<0.0005**	**<0.0005**
1.0° / 0.5°	LEACH	0.921	0.0105	**<0.0005**	**<0.0005**
1.0° / 0.3°	LEACH	**<0.0005**	**<0.0005**	0.185	0.354

Discussion

CLM Grid Scale Effect on Hydrology

The choice of grid resolution had a significant effect on estimate of volumetric soil water content, where lower resolutions predicted higher average soil moisture through all seasons (Figure 13b). Our results are similar to the findings of Freund & Kirchner (2017), Tesfa et al. (2016), and Shrestha et al. (2015; 2018) in that the spatial resolution influenced the available water content of the rooting zone. Scale errors manifested with increasing grid size in the results of Tesfa et al. (2014) as higher runoff (and therefore reduced soil water recharge), and as higher soil moisture and evapotranspiration in Freund& Kirchner (2017) and Shrestha et al. (2015, 2018).

In this research we note several processes related to grid scale effects on soil moisture. Broadly, topography is an important control on hydrologic cycle (Nijzink et al., 2016). In the Northeast US, topography exerts a strong influence on the partitioning of rainfall into runoff and infiltration, controlling soil moisture recharge (Buchanan et al., 2014; Easton et al., 2007), and the mobility of dissolved Nitrate (e.g. Knighton et al., 2017). The regional column approach to soil water recharge perhaps neglects the physical processes governing soil moisture recharge by representing rainfall-runoff partitioning as a predominantly infiltration-excess process, an issue previously discussed by Melsen et al. (2016). Decreasing the grid size from 1 to 0.3 degrees shows a drastic adjustment by the model in the spatial representation of soil moisture, providing direct evidence that this model applied to the HBEFwatershed is not achieving the "process-scale" (Bloschl & Sivapalan, 1995). The result directly shows issues of scale-dependent flux parameterization (e.g. Clark et al., 2015a; Beven et al., 2014) relevant to the adequate depiction of the local hydrologic conditions. Our research highlights the potential limitations of

process-based frameworks for regional hydrologic models given that there remain many open "process" questions in hydrology, such as the prevalence of infiltration-excess runoff regime across the US, or the appropriate numerical representation of denitrification (Groffman et al., 2009).

The energy balance of earth's land surface and canopy are similarly sensitive to grid scale which can exert a control on soil moisture (Shrestha et al., 2015) and therefore the N cycle. When controlling for atmospheric conditions, water availability in the rooting zone controls latent heat flux (e.g. Actual Evapotranspiration [AET]). Freund & Kirchner (2017) demonstrate this effect via simulated increased AET rates from progressively wetter soils at large grid scales. Shrestha et al. (2017) recorded a strong control by plants on ET rates in simulations with much finer resolutions. Given our discrepancy in soil moisture content, we would anticipate underestimation of AET from larger grid scales. Our results show that total ET (and therefore latent heat flux) did indeed change across resolutions at HBEF(Figure 19). While the total ET estimated across the model domain was well represented by the coarsest grid, the effects of spatially averaged latent heat flux could result in negative downstream effects on the hydrologic and N cycles. Similar to Shrestha et al. (2015) we demonstrate a scale-dependence of soil temperatures, suggesting further issues with the land surface energy balance.

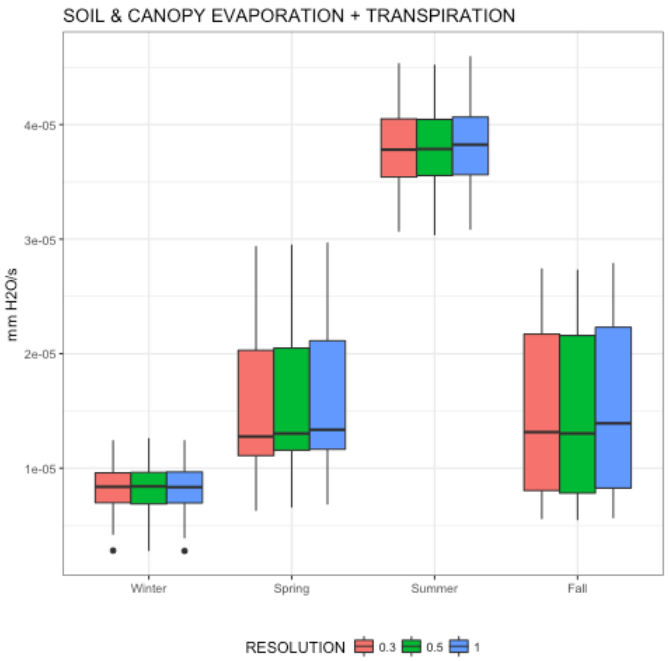

Figure 19 Total evapotranspiration fluxes. Differences between the scales are significantly greater than zero for all cases. The coarsest resolution had the higher fluxes on average. Center lines show the medians. Box limits indicate the 25th and 75th percentiles, with whiskers extending 1.5 times the interquartile range. Outliers are represented by dots.

CLM Grid Scale Effect on the Nitrogen Cycle

The choice of grid scale had a significant effect on the estimation of nitrification and leaching rates. We expected scaling differences in denitrification rates because of differences in soil moisture and anaerobic fraction, but the effect was less apparent. However, further analysis revealed modeled denitrification to be primarily sensitive to substrates (e.g. NH_4, NO_3, carbon) rather than abiotic factors like hydrology. The only exception was in the case of winter and spring nitrification when soil temperature was strongly correlated with nitrification rate. Furthermore, we expected the scaling effect to be greatest during the summer when soil moisture simulation with an uncalibrated model is difficult.

The lack of sensitivity to hydrology in the nitrification and denitrification modules was surprising. Denitrification is sensitive to soil moisture in many terrestrial models (Heinen, 2006, Tague, 2009). Field observations, where modeling ideas originate and are tested, also highlight the importance of soil moisture in determining nitrification and denitrification rates (Anderson et al., 2015). That soil moisture did not correlate with nitrification or denitrification in any of the seasons, raises suspicion that CLM's N cycle is not properly sensitive to abiotic factors. Certainly, it would be reasonable for a model to challenge the status quo, but we do not believe that was the intention in the design of this nitrification and denitrification submodel. If it were so, we expect the model to follow strategies used in the DNDC model, rather than Century. DNDC simulates changes in the soil denitrifier population to estimate denitrification rates (Li et al., 2000).

The choice of grid scale affected N leaching estimates much more strongly than nitrification and denitrification. Large differences in subsurface drainage rates across the scales led to seasonal differences in NO_3 leaching. The largest differences occurred in the winter and spring, when subsurface drainage limited the flux of NO_3 leached from the soil. The temporal drainage pattern during this period does not match the expected pattern of forested catchments. Drainage decreases as winter transitions to spring and reaches a minimum in April when surface runoff peaks. In all seasons, except a portion of the spring, drainage and runoff are positively correlated. In CLM, drainage volume is dependent on soil hydrologic properties that change with the soil organic fraction. In the case of our three resolutions, a higher soil organic fraction in the finest resolution decreased hydraulic conductivity and increased the water holding capacity of the soil. This is likely the reason the fine resolution has higher soil moisture content and lower

subsurface drainage. Differences in soil organic matter fraction originate during spin-up, when N and carbon accumulate more quickly in the finer resolutions. We spun up each model resolution for the same amount of time, rather than to the same mass of N in the soil stocks. Care should be exercised when comparing quantitative results between resolutions. Changes being made to the hydrology in CLM might also resolve the scalability problem in subsurface drainage (CLM5.0).

Extensions of this Research

Our research presents an estimate of the effect of model grid scale on the N cycle within the CLM4.5. Here we discuss some of the limitations of our work, opportunities for future research, and recommendations for progress on this topic.

The most common purpose of LSMs and ESMs is to provide an adequate working estimate of earth system processes at continental or global-scales, and to understand their influence on the global energy balance and general circulation. Our research considered issues of scale on the hydrologic and N cycles of a small region (8894 km^2) in the Northeast US, with a distinctly seasonal climate. In our numerical experiments, the model grid scale affected the energy, water, and N fluxes; however, we acknowledge that our results apply to this specific location, and we do not attempt to estimate the magnitude of this error at the operational scales of LSMs or ESMs. Additional research is required to estimate the effect of hydrologic and N cycle uncertainty on global climate sensitivity.

Our focus here was on potential issues in application of process-based models for hydrology and nutrient cycling when applied to regional horizontal grids. Process-based model evaluation as proposed by Melsen et al. (2016) suggests that we

should consider the relevant spatial and temporal scales when evaluating the usefulness of predictions of large scale hydrologic models. Rather than estimating N losses at global scales within ESMs it may therefore be most appropriate to push these models to high enough resolutions where plot- and hill-slope predictions of N cycling can be compared directly to the observational scale in-situ field experiments (e.g. Del Grosso et al., 2006).

We acknowledge the call for a universal framework based on a bottom-up approach to building process-based models at meaningful scales (e.g. Clark et al., 2015a, b); however, this is not necessarily the only relevant path towards resolving these issues of scale. ESMs are based on physical relationships where possible (e.g. energy and mass balances), and yet remain dependent on highly parameterized routines because of open questions in hydrology and biogeochemistry (e.g. Groffman et al., 2009). Emerging methods in probabilistic treatment of uncertain hydrologic model parameterizations (e.g. Orth et al., 2016) and continental scale calibration (e.g. Abbaspour et al., 2015) may help to constrain processes at the more relevant prediction-scale where process-based modeling is not yet feasible.

A simplification of the anaerobic fraction calculation utilized by the denitrification and methane models may address the lack of coupling between the hydrologic and N cycles. It is common in models at the watershed to regional scale to represent anoxic conditions with soil moisture status, rather than to explicitly calculate the anoxic conditions directly from ongoing biological processes (Heinen, 2006). It is more difficult to measure (and thus check the model) soil respiration than soil moisture. Measurements of soil moisture are also far more prevalent at several spatial scales, making it a better proxy for anoxic soil conditions and modeling denitrification. We can make concrete headway on improving representation of soil

moisture at large scales that wouldn't be possible with a nonlinear, spatially and temporally heterogeneous state like anoxic fraction.

Conclusion

We found that the choice in grid scale affected model estimates of soil moisture, nitrification, nitrate leaching, and to a lesser degree, denitrification. Our results indicate the N modules may not be accurately representing the coupled nature of the terrestrial hydrology and N cycles. Further, if adjustments are made that reflect the strong relationship between denitrification and soil moisture, it is likely the difference in denitrification across scales will increase. Leaching estimates are scale dependent and therefore modelers should be careful when interpreting results. The recommended spin-up procedure will generate different soil hydraulic properties for a model resolution, resulting in different drainage and runoff rates. Moving forward, it is recommended that the hydrology scaling problem be reevaluated under the changes implemented in CLM5 and upon improvements, the N cycle be more closely coupled to the hydrologic cycle.

LITERATURE CITED

Abbaspour, K. C., Rouholahnejad, E., Vaghefi, S., Srinivasan, R., Yang, H., & Kløve, B. (2015). A continental-scale hydrology and water quality model for Europe: Calibration and uncertainty of a high-resolution large-scale SWAT model. *Journal of Hydrology*, *524*, 733–752. http://doi.org/10.1016/j.jhydrol.2015.03.027

Anderson, T. R., Groffman, P. M., & Walter, M. T. (2015). Using a soil topographic index to distribute denitrification fluxes across a northeastern headwater catchment. *Journal of Hydrology*, *522*, 123–134. http://doi.org/10.1016/j.jhydrol.2014.12.043

Arneth, A., Harrison, S. P., Zaehle, S., Tsigaridis, K., Menon, S., Bartlein, P. J., … Vesala, T. (2010). Terrestrial biogeochemical feedbacks in the climate system. *Nature Geoscience*, *3*(8), 525–532. http://doi.org/10.1038/ngeo905

Arora, V. K., Boer, G. J., Friedlingstein, P., Eby, M., Jones, C. D., Christian, J. R., … Wu, T. (2013). Carbon–Concentration and Carbon–Climate Feedbacks in CMIP5 Earth System Models. *Journal of Climate*, *26*(15), 5289–5314. http://doi.org/10.1175/JCLI-D-12-00494.1

Bernhardt, E. S., Blaszczak, J. R., Ficken, C. D., Fork, M. L., Kaiser, K. E., & Seybold, E. C. (2017). Control Points in Ecosystems: Moving Beyond the Hot Spot Hot Moment Concept. *Ecosystems*. http://doi.org/10.1007/s10021-016-0103-y

Blöschl, G., & Sivapalan, M. (1995). Scale issues in hydrological modelling: A review. *Hydrological Processes*, *9*(3–4), 251–290. http://doi.org/10.1002/hyp.3360090305

Bonan, G. B., & Levis, S. (2010). Quantifying carbon-nitrogen feedbacks in the Community Land Model (CLM4). *Geophysical Research Letters*, *37*(7), n/a-n/a. http://doi.org/10.1029/2010GL042430

Boyer, E. W., Alexander, R. B., Parton, W. J., Li, C., Butterbach-Bahl, K., Donner, S. D., … Grosso, S. J. Del. (2006). Modeling Denitrification in Terrestrial and Aquatic Ecosystems At Regional Scales. *Ecological Applications*, *16*(6), 2123–2142. http://doi.org/10.1890/1051-0761(2006)

Buchanan, B. P., Fleming, M., Schneider, R. L., Richards, B. K., Archibald, J., Qiu, Z., & Walter, M. T. (2014). Evaluating topographic wetness indices across central New York agricultural landscapes. *Hydrology and Earth System Sciences*, *18*(8), 3279–3299. http://doi.org/10.5194/hess-18-3279-2014

Butterbach-Bahl, K., Stange, F., Papen, H., & Li, C. (2001). Regional inventory of nitric oxide and nitrous oxide emissions for forest soils of southeast Germany using the biogeochemical model PnET-N-DNDC. *Journal of Geophysical Research: Atmospheres*, *106*(D24), 34155–34166. http://doi.org/10.1029/2000JD000173

Clark, M. P., Nijssen, B., Lundquist, J. D., Kavetski, D., Rupp, D. E., Woods, R. A., … Rasmussen, R. M. (2015). A unified approach for process-based hydrologic modeling: 1. Modeling concept. *Water Resources Research*, *51*(4), 2498–2514. http://doi.org/10.1002/2015WR017198

Clark, M. P., Nijssen, B., Lundquist, J. D., Kavetski, D., Rupp, D. E., Woods, R. A., … Marks, D. G. (2015). A unified approach for process-based hydrologic modeling: 2. Model implementation and case studies. *Water Resources Research*, *51*(4), 2515–2542. http://doi.org/10.1002/2015WR017200

Del Grosso, S. J., Parton, W. J., Mosier, A. R., Walsh, M. K., Ojima, D. S., & Thornton, P. E. (2006). DAYCENT National-Scale Simulations of Nitrous Oxide Emissions from Cropped Soils in the United States. *Journal of Environmental Quality*, *35*(4), 1451. http://doi.org/10.2134/jeq2005.0160

Easton, Z. M., Gérard-Marchant, P., Walter, M. T., Petrovic, a. M., & Steenhuis, T. S. (2007). Hydrologic assessment of an urban variable source watershed in the northeast United States. *Water Resources Research*, *43*(3), n/a-n/a. http://doi.org/10.1029/2006WR005076

Fatichi, S., Pappas, C., & Ivanov, V. Y. (2016). Modeling plant-water interactions: an ecohydrological overview from the cell to the global scale. *Wiley Interdisciplinary Reviews: Water*, *3*(3), 327–368. http://doi.org/10.1002/wat2.1125

Friedlingstein, P., Cox, P., Betts, R., Bopp, L., von Bloh, W., Brovkin, V., … Zeng, N. (2006). Climate–Carbon Cycle Feedback Analysis: Results from the C 4 MIP Model Intercomparison. *Journal of Climate*, *19*(14), 3337–3353. http://doi.org/10.1175/JCLI3800.1

Galloway, J. N., Dentener, F. J., Capone, D. G., Boyer, E. W., Howarth, R. W., Seitzinger, S. P., … Voosmarty, C. J. (2004). Nitrogen Cycles: Past, Present, and Future. *Biogeochemistry*, *70*(2), 153–226. http://doi.org/10.1007/s10533-004-0370-0

Groffman, P. M., Davidson, E. A., & Seitzinger, S. (2009). New approaches to modeling denitrification. *Biogeochemistry*, *93*(1–2), 1–5. http://doi.org/10.1007/s10533-009-9285-0

Gruber, N., & Galloway, J. N. (2008). An Earth-system perspective of the global nitrogen cycle. *Nature*, *451*(7176), 293–296. http://doi.org/10.1038/nature06592

Heinen, M. (2006). Simplified denitrification models: Overview and properties. *Geoderma*, *133*(3–4), 444–463. http://doi.org/http://dx.doi.org/10.1016/j.geoderma.2005.06.010

Houlton, B. Z., Marklein, A. R., & Bai, E. (2015). Representation of nitrogen in climate change forecasts. *Nature Climate Change*, *5*(5), 398–401. http://doi.org/10.1038/nclimate2538

Kirchner, J. W. (2006). Getting the right answers for the right reasons: Linking measurements, analyses, and models to advance the science of hydrology. *Water Resources Research*, *42*(3). http://doi.org/10.1029/2005WR004362

Knighton, J. O., DeGaetano, A., & Walter, M. T. (2017). Hydrologic State Influence on Riverine Flood Discharge for a Small Temperate Watershed (Fall Creek, United States): Negative Feedbacks on the Effects of Climate Change. *Journal of Hydrometeorology*, *18*(2), 431–449. http://doi.org/10.1175/JHM-D-16-0164.1

Koven, C. D., Riley, W. J., Subin, Z. M., Tang, J. Y., Torn, M. S., Collins, W. D., … Swenson, S. C. (2013). The effect of vertically resolved soil biogeochemistry and alternate soil C and N models on C dynamics of CLM4. *Biogeosciences*, *10*(11), 7109–7131. http://doi.org/10.5194/bg-10-7109-2013

Lawrence, D. M., Oleson, K. W., Flanner, M. G., Thornton, P. E., Swenson, S. C., Lawrence, P. J., … Slater, A. G. (2011). Parameterization improvements and functional and structural advances in Version 4 of the Community Land Model. *Journal of Advances in Modeling Earth Systems*, *3*(1), n/a-n/a. http://doi.org/10.1029/2011MS00045

Li, C., Aber, J., Stange, F., Butterbach-Bahl, K., & Papen, H. (2000). A process-oriented model of N ₂ O and NO emissions from forest soils: 1. Model development. *Journal of Geophysical Research: Atmospheres*, *105*(D4), 4369–4384. http://doi.org/10.1029/1999JD900949

Likens, G. E. (2013). *Biogeochemistry of a forested ecosystem*. Springer Science & Business Media.

Melsen, L. A., Teuling, A. J., Torfs, P. J. J. F., Uijlenhoet, R., Mizukami, N., & Clark, M. P. (2016). HESS Opinions: The need for process-based evaluation of large-domain hyper-resolution models. *Hydrology and Earth System Sciences*, *20*(3), 1069–1079. http://doi.org/10.5194/hess-20-1069-2016

Morse, J. L., Durán, J., & Groffman, P. M. (2015). Soil Denitrification Fluxes in a Northern Hardwood Forest: The Importance of Snowmelt and Implications for Ecosystem N Budgets. *Ecosystems*, *18*(3), 520–532. http://doi.org/10.1007/s10021-015-9844-2

Nijzink, R. C., Samaniego, L., Mai, J., Kumar, R., Thober, S., Zink, M., … Hrachowitz, M. (2016). The importance of topography-controlled sub-grid process heterogeneity and semi-quantitative prior constraints in distributed hydrological models. *Hydrology and Earth System Sciences*, *20*(3), 1151–1176. http://doi.org/10.5194/hess-20-1151-2016

Oleson, K. W., Niu, G.-Y., Yang, Z.-L., Lawrence, D. M., Thornton, P. E., Lawrence, P. J., … Qian, T. (2008). Improvements to the Community Land Model and their impact on the hydrological cycle. *Journal of Geophysical Research: Biogeosciences*, *113*(G1), n/a-n/a. http://doi.org/10.1029/2007JG000563

Orth, R., Dutra, E., & Pappenberger, F. (2016). Improving Weather Predictability by Including Land Surface Model Parameter Uncertainty. *Monthly Weather Review*, *144*(4), 1551–1569. http://doi.org/10.1175/MWR-D-15-0283.1

Pachauri, R. K., Allen, M. R., Barros, V. R., Broome, J., Cramer, W., Christ, R., … others. (2014). *Climate change 2014: synthesis report. Contribution of Working Groups I, II and III to the fifth assessment report of the Intergovernmental Panel on Climate Change*. IPCC.

Parton, W. J., Stewart, J. W. B., & Cole, C. V. (1988). Dynamics of C, N, P and S in grassland soils: a model. *Biogeochemistry*, *5*(1), 109–131. http://doi.org/10.1007/BF02180320

Prather, M. J., Derwent, R., Ehhalt, D., Fraser, P. J., Sanhueza, E., & Zhou, X. (1995). Other trace gases and atmospheric chemistry. In *Climate change 1994: radiative forcing of climate change an evaluation of the IPCC IS92 emission scenarios* (pp. 73–126). Cambridge: Cambridge University Press. Retrieved from https://publications.csiro.au/rpr/pub?list=BRO&pid=procite:e43a8997-75f3-4a32-8125-e1fe34ca1afc

Rouholahnejad Freund, E., & Kirchner, J. W. (2017). A Budyko framework for estimating how spatial heterogeneity and lateral moisture redistribution affect average evapotranspiration rates as seen from the atmosphere. *Hydrology and Earth System Sciences*, *21*(1), 217–233. http://doi.org/10.5194/hess-21-217-2017

Schwarz, P. A., Fahey, T. J., & McCulloch, C. E. (2003). Factors Controlling Spatial Variation Of Tree Species Abundance In A Forested Landscape. *Ecology*, *84*(7), 1862–1878. Retrieved from http://onlinelibrary.wiley.com/doi/10.1890/0012-9658

Shrestha, P., Sulis, M., Simmer, C., & Kollet, S. (2018). Effects of horizontal grid resolution on evapotranspiration partitioning using TerrSysMP. *Journal of Hydrology*. http://doi.org/https://doi.org/10.1016/j.jhydrol.2018.01.024

Shrestha, P., Sulis, M., Simmer, C., & Kollet, S. (2015). Impacts of grid resolution on surface energy fluxes simulated with an integrated surface-groundwater flow model. *Hydrology and Earth System Sciences*, *19*(10), 4317–4326. http://doi.org/10.5194/hess-19-4317-2015

Soil Survay Staff. (2006). *Keys to soil taxonomy*. Washington, DC.

Tague, C. (2009). Modeling hydrologic controls on denitrification: sensitivity to parameter uncertainty and landscape representation. *Biogeochemistry*, *93*(1–2), 79–90. http://doi.org/10.1007/s10533-008-9276-6

Tesfa, T., Leung, L. R., Huang, M., Li, H.-Y., Voisin, N., & Wigmosta, M. S. (2014). Scalability of grid-land subbasin-based land surface modeling approaches for hydrologic simulations. *Journal of Geophysical Research*, (3), 1–19. http://doi.org/10.1002/2013JD02049.

Thomas, R. Q., Zaehle, S., Templer, P. H., & Goodale, C. L. (2013). Global patterns of nitrogen limitation: Confronting two global biogeochemical models with observations. *Global Change Biology*, *19*(10), 2986–2998. https://doi.org/10.1111/gcb.12281

Viovy, N. (2011). CRUNCEP Dataset. Retrieved from http://dods.extra.cea.fr/store/p529viov/cruncep

Vitousek, P. M., Aber, J. D., Howarth, R. W., Likens, G. E., Matson, P. A., Schindler, D. W., … Tilman, D. G. (1997). Human Alteration of the Global Nitrogen Cycle: Sources and Consequences. *Ecological Applications*, *7*(3), 737–750. http://doi.org/10.1890/1051-0761(1997)007

Wieder, W. R., Grandy, A. S., Kallenbach, C. M., Taylor, P. G., & Bonan, G. B. (2015). Representing life in the Earth system with soil microbial functional traits in the MIMICS model. *Geoscientific Model Development*, *8*(6), 1789–1808. http://doi.org/10.5194/gmd-8-1789-2015

Zaehle, S., & Dalmonech, D. (2011). Carbon–nitrogen interactions on land at global scales: current understanding in modelling climate biosphere feedbacks. *Current Opinion in Environmental Sustainability*, *3*(5), 311–320. http://doi.org/10.1016/j.cosust.2011.08.008

Zak, D. R., Tilman, D., Parmenter, R. R., Rice, C. W., Fisher, F. M., Vose, J., … Martin, C. W. (1994). Plant production and soil microorganisms in late-successional ecosystems: A continental-scale study. *Ecology*, *75*(8), 2333–2347.

CHAPTER 3
DENITRIFYING BIOREACTOR PERFORMANCE UNDER VARYING FLOW CONDITIONS

Introduction

Denitrifying bioreactors (bioreactors) installed at the edge of agricultural fields remove nitrate from tile drainage water in an incredibly simple design, but fine tuning their performance is difficult. Nitrate-rich water traveling through tile drains arrives at the bioreactor in varying flowrates, temperatures, and concentrations, all which impact nitrate removal performance.

Nitrate removal rate and removal efficiency are two performance metrics commonly used to assess and improve engineered designs. Removal rate, expressed in units of mass per volume per time, is the difference between the incoming and outgoing nitrate load, normalized by the bioreactor volume. Typical removal rates for field bioreactors range between 3 and 7 gN m^{-3} d^{-1}(Addy et al., 2016). Bioreactor removal efficiency is a measure of the mass of nitrate removed divided by the incoming load. While operation at 100% efficiency is desirable, field woodchip bioreactors have dipped below 25% (Christianson et al., 2012). In some studies, efficiency is calculated from concentration, rather than load. In the regulatory context of a Total Maximum Daily Load, annual nitrate export is the important metric for evaluating water treatment technology.

Scientific studies of laboratory and field bioreactors find that performance strongly correlates with the length of time the nitrate-rich water spends migrating through the bioreactor. Reviews of many bioreactors show that hydraulic retention times (HRT) correlate with both removal rate (Christianson et al., 2012, Addy et al., 2016) and removal efficiency (Hoover et al. 2016). From this finding, mechanistic

models have used HRT to effectively predict the concentration of nitrate removed (Ghane et al., 2015, Halaburka et al., 2017). Engineered designs focus on maintaining an appropriate hydraulic retention time (HRT) by installing flow control structures (e.g. Hassanpour et al., 2017) and adjusting bioreactor size (Christianson et al., 2011). The bioreactor must be designed to produce HRTs that are neither too short, nor long—evidence suggests that N limited conditions can produce harmful byproducts like methyl mercury, among others (Addy et al., 2016). Design approaches, emphasize balancing the need to treat most of the drainage water with space constraints and the deleterious effects of long HRTs (Christianson et al., 2011).

Variation in flow rates during storm events adds to the complication in designing bioreactors for the optimal HRT. Rainfall intensity, duration, and antecedent moisture conditions create a range of hydraulic flows in tile drains (Lam et al., 2016). Coupled with soil hydraulic properties and tile drainage areas, the design of a bioreactor for a set of HRTs is a very site specific endeavor. Few studies have specifically evaluated the performance of woodchip bioreactors during storm events. Moorman et al. (2015) found evidence that storm event removal rates were different from rates during baseflow conditions. To further complicate bioreactor performance, storm events not only change flowrates, but also introduce rapid changes in water temperature and nitrate conditions. Temperature is an important control on denitrification, and has explained a sizable portion of bioreactor removal rate variation in previous field studies (Schmidt & Clark, 2013; Hoover et al., 2016). Removal rates decline as influent nitrate concentrations decrease and create N limiting conditions where the reaction is controlled by factors other than nitrate availability (see meta-analysis by Addy et al., 2016).

Our objective in this study was to investigate how shifts in flow rates, and subsequently HRT, experienced during storm events would impact the total removal of nitrate in a bioreactor. More data on bioreactor performance during storms is needed to understand the relative influence of these variables, but data collection is difficult. Empirical research in this area is ongoing (Pluer et al., 2019), but to provide usable design information for addressing a range of bioreactor flow rates, we present this exploration of flow variability and bioreactor performance using synthetic data modeled after observed flow distributions in an existing woodchip bioreactor in central New York. This analysis provided a preliminary assessment for designing bioreactors in anticipation of hydrologic changes that may occur as results of land use or climate change.

Methods

Field Bioreactor Conditions

We used data collected at bioreactors located in Chemung and Tompkins Counties in central New York State. Two bioreactors were constructed on each site in 2013 and 2012 and operate in parallel receiving the same influent water. Woodchips were mixed with biochar at a 9:1 volumetric ratio in one bioreactor, while the other was filled with woodchips only. The Chemung bioreactors receive water draining a corn field with silty loam soils that is approximately 5 hectares in size. Manure was applied to the corn field twice a growing season—in the spring and the fall. Influent nitrate concentration averaged 1.4 mg N L^{-1}. The bioreactors in Tompkins County have a drainage area of 2 hectares where vegetable crops are grown using inorganic fertilizer. Average influent nitrate concentration were 2.1 mg N L^{-1}. The sites received approximately 900 mm of rainfall during the study focal years of 2014-2015, close to the 100-year annual average. Further details on the climatic conditions, bioreactor construction, and calculation of flow rates is available in

Hassenpour et al. (2017).

The bioreactors are fitted with flow boxes at their entrances and exits and they maintain saturated conditions for a minimum volume of 9455 L, except for the woodchip+biochar bioreactor in Chemung County. That bioreactor is larger than the other three– 17100 L. The flow boxes also facilitate the collection of flow data. From April to November 2015, HOBO® U20 water level loggers recorded the height of water from inside the inlet and outlet flow boxes. Flowrate (L s^{-1}) through the bioreactors was calculated using a standard equation for a sharp crested weir,

$$Q = C_w H^{1.4856}$$

where H is the height of the water above the weir (cm). The weir coefficient, C_w was determined empirically to be 0.3255 (Hassanpour et al., 2017). Flowrate was used to determine HRT for each record. We used a common theoretical equation for HRT in horizontal bed bioreactors.

$$HRT = \frac{V_s n_e}{Q}$$

where V_s is the saturated volume of the bioreactor and n_e the effective porosity. To simplify analysis, we considered V_s and n_e to be constant in our bioreactors, such that HRT is only function of the flowrate Q. To date, we know of no evidence to consider n_e dynamic over a storm event. The shift in V_s is small and is constrained by the height of the inlet and outlet flow boxes.

Model Bioreactor Design

The flowrate dataset from the 2014 and 2015 growing seasons were used to define the shape and spread of simulated datasets. 100 simulated flow rate scenarios were generated from the gamma distribution using the statistics package in R version 3.3.3 (R Core Team, 2017). Gamma distribution shape and scale parameters were

randomly assigned to give a variety of flow scenarios that could be used to compare hydrologic conditions to bioreactor performance (Table 1). The volume of water and concentration of nitrate entering the bioreactor were held constant in every scenario. To do this, the number of non-zero flow events varied, i.e., a bioreactor receiving water from a few high flow events had fewer records than one with many low flow events. The number of records in each scenario varied between 10,000 and 50,000. Entering nitrate concentrations were set at 6 mg N L^{-1}, the median concentration measured in the field bioreactors during storm events.

HRT was calculated using the above equation and applied to a zero-order nitrate reduction model (Halaburka et al., 2017). The simple model is

$$N = N_o - V_N HRT$$

where N is the ending nitrate concentration (mg N L^{-1}), No is influent concentration (1.3 mg N L^{-1}), and V_N is the zero-order denitrification rate (mg N^{-1} h^{-1}). This model was the best predictor of nitrate reduction in a comparison of five mechanistic models of lab bioreactors under constant temperature and flow conditions. In the experiment, sampling ports along the length of the column were used to measure nitrate conditions that translated to HRTs between 0.6 to 36 hours. Simulated HRTs in this study were kept under 40 hours, although higher HRTs have been recorded in the field.

We selected the appropriate denitrification rate parameter value and compared the model's predicted outflow concentrations to measurements from 108 grab samples taken from the Tompkins and Chemung bioreactors. The samples were taken sporadically between March 2013 and October 2015. Measured inflow concentrations ranged from 0 to 20 mg N L^{-1}, but due to the model limitations noted by Halaburka et al., (2017), we omitted 6 measurements with concentrations

less than 2 mg N L^{-1}. At low concentrations, nitrate removal in a woodchip bioreactor can no longer be characterized as a zero order reaction. We compared model performance for each denitrification rate parameter using the coefficient of determination and selected the highest performing model.

Using this model, we calculated outflow nitrate concentrations and nitrate export for each of the simulated flow scenarios. We computed summary statistics and the total nitrate export for each flow scenario.

Table 5 Parameter values and ranges for all flow scenarios

Effective Porosity	Bioreactor Saturated Volume	Total Discharge	Gamma Shape Parameter	Gamma Scale Parameter	Inflow Nitrate Concentration	Denitrification Rate Parameter
-	*L*	*L*	*L* s^{-1}	*L* s^{-1}	*mg N* L^{-1}	*mg N* L^{-1} h^{-1}
0.6	9455	9455	5-10	0.5-10	6.0	0.4

Results & Discussion

Model Performance

The best fit to empirical data was achieved with a denitrification rate parameter value of 0.4 and 0.45 mg N L^{-1} h^{-1} for the Tompkins and Chemung County bioreactors, respectively. The model performed reasonably well in predicting outflow nitrate concentrations (Figure 20), but less so when the highest concentration value of 12.5 mg N L^{-1} was removed from the dataset. In model testing, Halaburka et al. (2015) did not vary water temperature, an important factor of denitrification. We expect that a portion of the variation in the observed outflow concentrations is attributable to the temperature fluctuation in our bioreactors. Water temperature ranged from 3º to 18º C. Other bioreactor studies identify a correlation between removal rate and water temperature (e.g. Hoover et al., 2016) and most process-based models of denitrification include a temperature factor (Heinen, 2006).

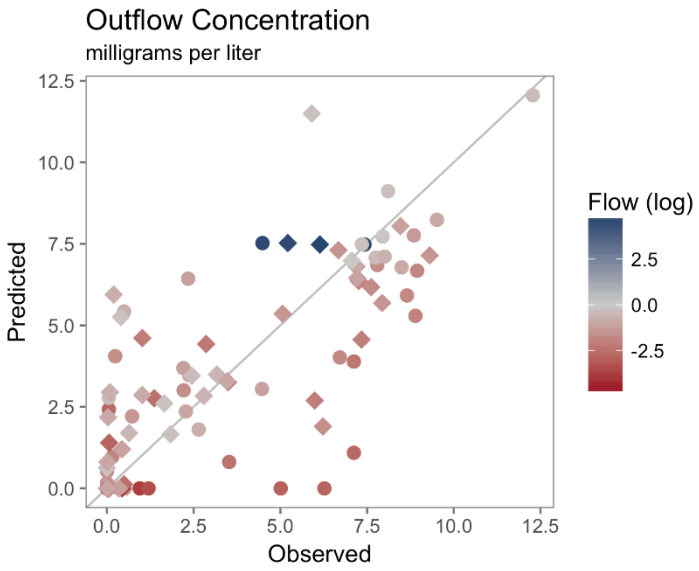

Figure 20 Comparison of observed and modeled outflow nitrate concentrations at Tompkins and Chemung County DNBRs for grab samples taken between 2013 and 2015. The grey line is the 1:1 line indicating perfect predictions. Circles represent woodchip bioreactors and diamonds are woodchip plus biochar bioreactors. The color gradient indicates higher flows in blue and lower flows in red.

Flowrate Evaluation

The flow distributions from the four field bioreactors had different peaks and varied in spread. The flow distributions at each site varied between the two seasons and the Tompkins County bioreactors had lower flowrates due to their smaller drainage area (Figure 21).

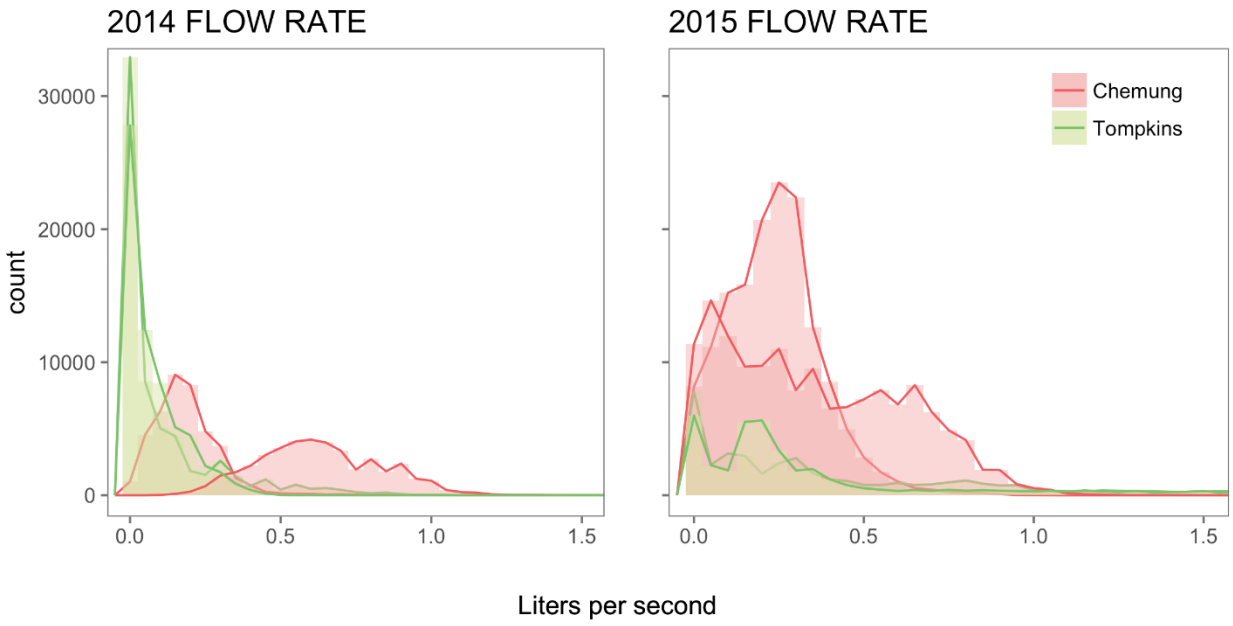

Figure 21 Empirical flow distributions of four DNBRs during the 2014 and 2015 growing seasons. One woodchip and one woodchip+biochar bioreactors are located at each site.

The empirical flow distributions were used to inform the distribution characteristics of the 100 simulated flow scenarios. Four representative flow distribution scenarios and their corresponding HRT distributions are shown in Figure 22.

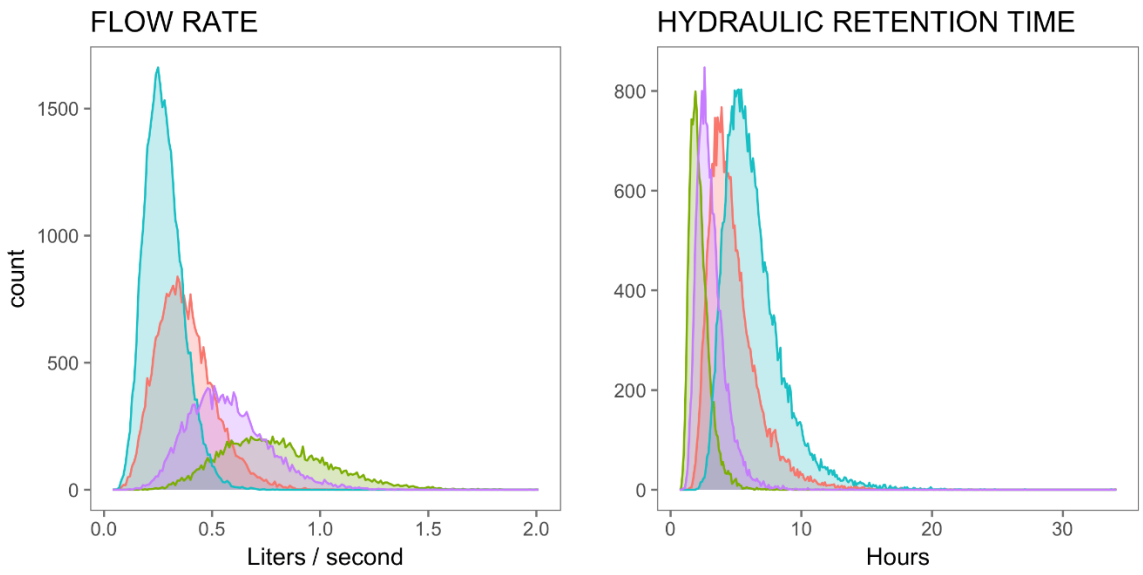

Figure 22 Histograms of sample distributions of flow rate and their corresponding hydraulic retention times. Scenarios with a high proportion of low flows have longer hydraulic retention times. The sum of the flows in each scenario (i.e. the area under the curve) is equivalent. The sum of the hydraulic retention times is not.

Using the concentration model, we relate nitrate export (NE) at a specific time to HRT (Figure 23). When we assume that incoming and outgoing flow rate from the bioreactor is the same, NE becomes

$$NE = (N - V_N HRT) * Q$$

In large field bioreactors, the incoming and outgoing flow rates can differ slightly depending on outlet design. We assume this difference is negligible and lasts only for a short period of time in our bioreactor, but sensitivity to this assumption is an avenue for further exploration.

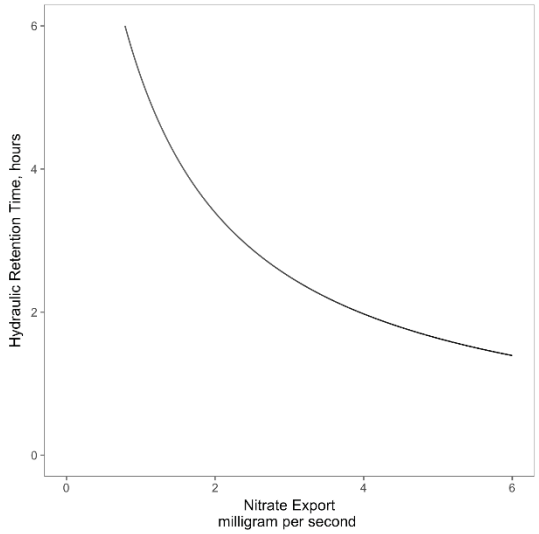

Figure 23 Nitrate export decreases exponentially as the hydraulic retention time increases, according to the zero-order mechanistic model by Halaburka et al. (2015).

Each flow scenario produced a NE distribution that closely matched the shape of the flow distribution (Figure 24).

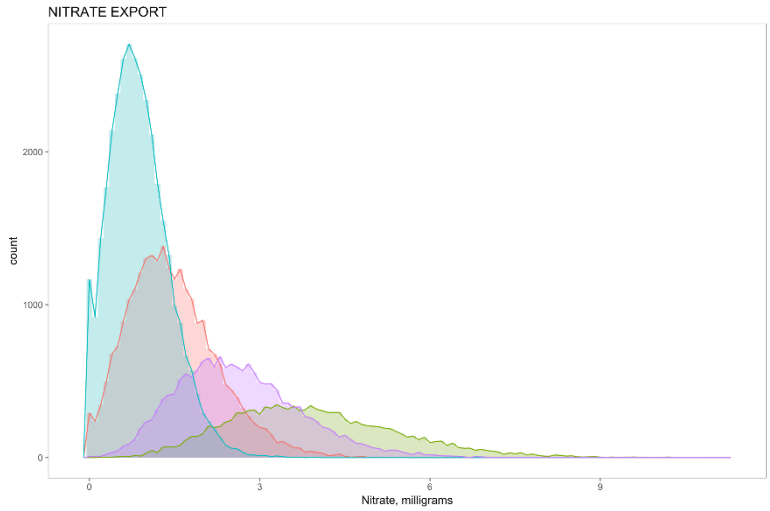

Figure 24 Histogram of nitrate export for four example flow scenarios. Although the same mass of nitrate was introduced, the scenarios have different numbers of non-zero flow events and sum to different total export values.

Unlike the flow distributions, the area under the nitrate export curves differed. This

area, or the sum of the exports from several flow events, we refer to as the total nitrate export (TNE). For a series of events over time, the sum of these discrete exports combined with the theoretical HRT equation, simplify to

$$TNE = \sum_{i=1}^{n} N_o\, Q_i - n(V_N V_s n_e)$$

By using the same flow volume and a constant concentration, we ensured the mass of nitrate entering the bioreactor was the same in all scenarios. The first term in the above equation is then a constant across all scenarios and TNE in any one scenario is proportional to the number of non-zero flow events in the record. TNE increases as the number of flow events decreases, independent of the maximum flow event size within a scenario (Figure 25).

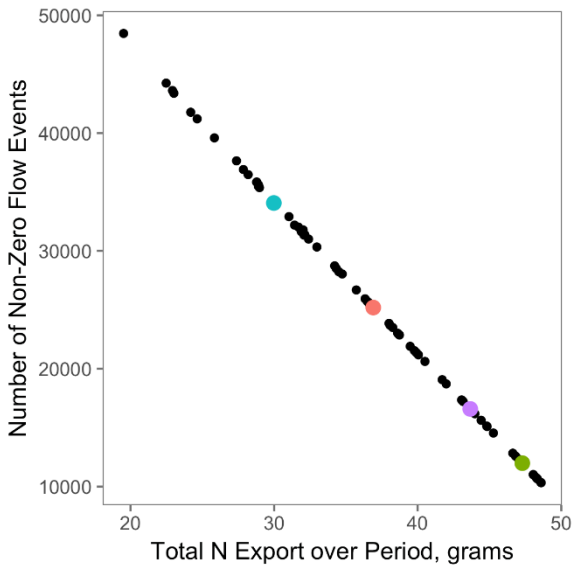

Figure 25 Relationship of total nitrate export and number of non-zero flow events in each scenario. As the number of non-zero flow events decreases, corresponding to an increase in the number of higher flow events, the total nitrate export increases. The black points are data from all scenarios and the points in color correspond to the example scenarios in Figures 22 and 24.

Practical application of this finding is limited, given the unlikely possibility

of controlling of the number of precipitation-driven flow events experienced by a bioreactor. Instead, this finding anchors the prevailing idea that consistent, small inputs to the bioreactor is preferable to a few large flow events. If flow to the bioreactor is expected to be flashy and cannot be managed before entering the bioreactor, increasing the bioreactor volume will reduce TNE. Bioreactor design guidance reflects this idea.

In the design case where flow to the bioreactor can be managed, with inlet control gates or tile drain management, reduction to a lower average flow rate will reduce TNE. In our simulations, we related mean and median flow rate to TNE (Figure 26) using an exponential model of the form

$$y = e^{a+bx}$$

where y is the flow rate statistic in liters per second and x is TNE in grams. Table 6 provides the fitted values for the parameters and the adjusted R^2.

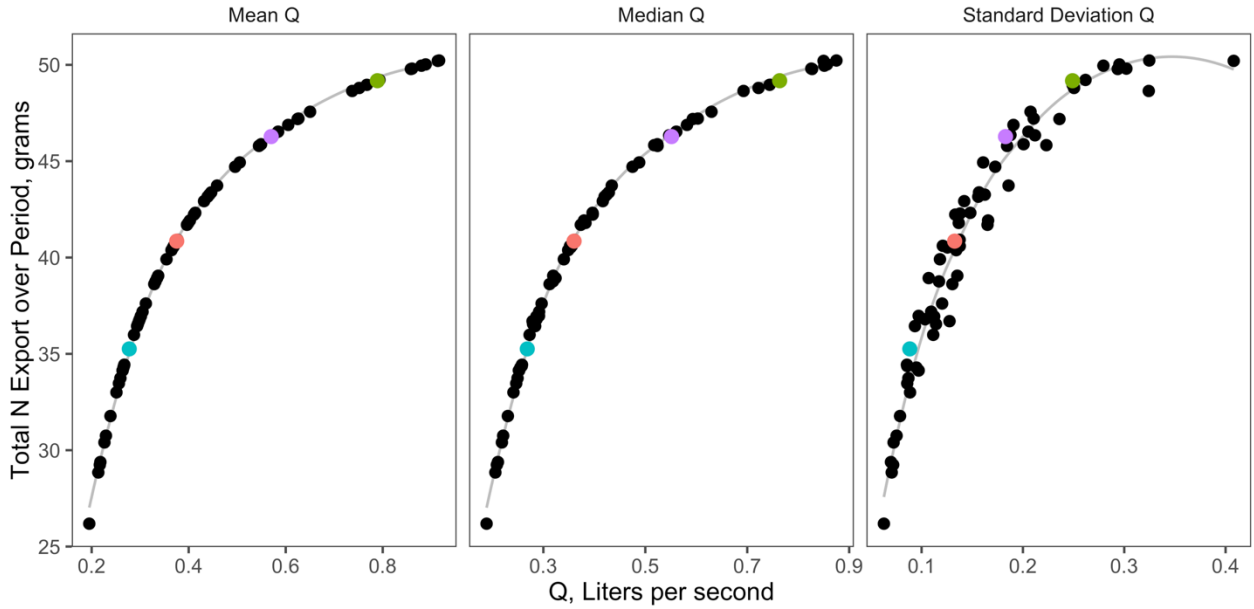

Figure 26 Total nitrate export for all flow scenarios plotted against mean, median, and standard deviation of flow rates. The points in color correspond to scenarios highlighted in Figures 22, 24, and 25. Refer to Table 6 for fitted parameter values of the fitted grey line.

Table 6 Fitted Exponential Model Parameter values for all flow scenarios

Flow Rate Statistic	Coefficient a	Coefficient b	Adjusted R^2
Mean	-4.19	0.0799	0.966
Median	-4.23	0.0799	0.966
Standard Deviation	-5.23	0.0797	0.909

For scenarios with flow rates, a 25% reduction in the mean flow rate will result in approximately 10% less TNE. The same percent reduction at lower flow rates reduces TNE even more—about 15% of the original mass of nitrate.

The flow statistic-export relationship in Figure 26 considers only the non-zero flow events. When flow scenario statistics are recalculated after assigning zero values to flow and NE for the remainder of the record (n=50,000 for all scenarios), a different flow statistic-export relationship emerges. Mean flow is no longer relevant (the flow scenarios still sum to the same discharge volume), but standard deviation becomes an important indicator of TNE. The four representative scenarios are presented in Figure 27. The takeaway is still the same though—a larger number of low flow events is preferable for minimizing TNE.

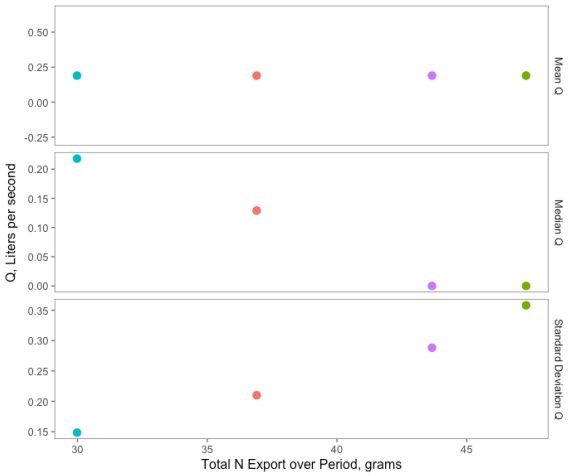

Figure 27 Total nitrate export where the four scenarios were extended to 50,000 records with flow and export values equal to zero.

The results of this analysis and the flow statistic-export relationship are highly sensitive to the denitrification rate parameter, V_n in the concentration model. We used the value suggested by Halaburka et al. (2017) as the median literature value, but the range documented is between 0.05 and 2.0 mg N L^{-1} h^{-1}. A brief sensitivity analysis demonstrated that adjustments in V_n produce different flow statistic-export relationships (Figure 28), therefore we suggest selecting a parameter value that reflects site or regional conditions. The parameter is a placeholder for rate limiting conditions such as temperature and carbon availability. Under steady conditions, like the laboratory experiments used to test the concentration model, a single value is acceptable. In reality, field bioreactors experience sharp temperature changes. Temperature variation could be introduced to the concentration model through the denitrification rate parameter or by adding a scaling term defined by a Van't Hoff-Arrhenius function (Ghane et. al, 2015). Correlating temperature with flowrate (simulating for instance, cooler water delivered in a summer storm) could produce more realistic set of bioreactor conditions.

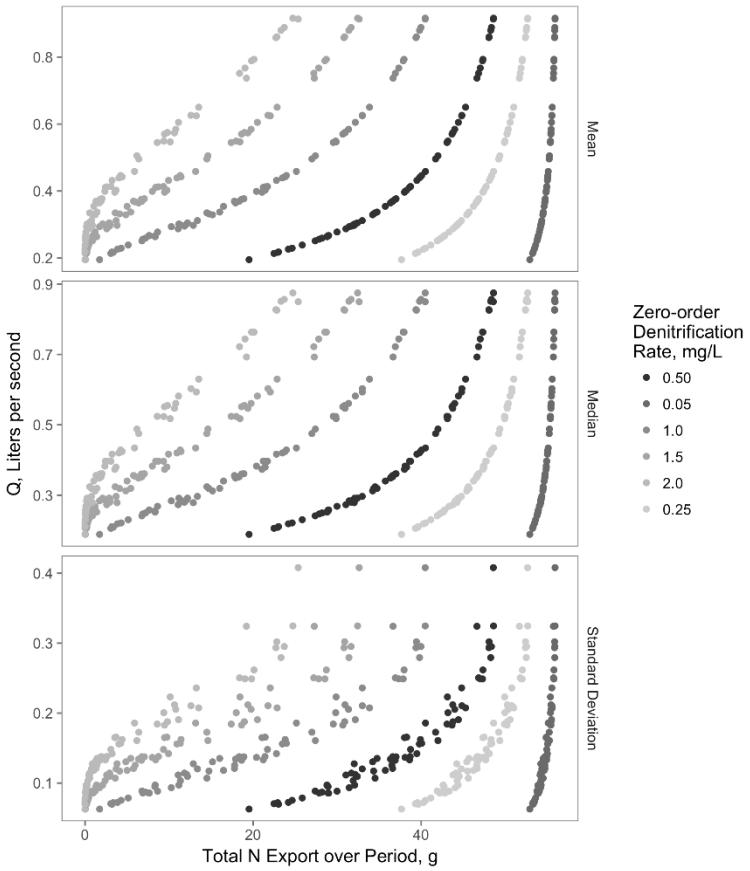

Figure 28 Total nitrate export results are sensitive to the zero-order denitrification parameter. The median value of 0.4 was used elsewhere in this study.

High frequency monitoring of nitrate concentrations in agricultural watersheds has shown to both increase and decrease during storm events, depending on the nutrient supply, season, and antecedent conditions (Wade et al., 2012). In this analysis, we maintained a constant inflow concentration of 6 mg N L^{-1}, but future work could allow concentrations to vary according to a discharge-concentration relationship that is based on the expected nitrate supply of the drainage area. With high-frequency nitrate-nitrite measurements, Jones et al. (2017) developed a promising analytical method for approximating the nitrate-nitrite concentration-discharge relationship in a tile drained watershed. They found that during wet parts of the year, soil nitrate supplies could be depleted, resulting in

a “turning point” in the concentration-discharge pattern. Further work on our flow distribution analysis could incorporate a dynamic concentration value based on their findings.

The saturated volume of the bioreactor is another important input in this analysis. Decreasing or increasing the size of the bioreactor by 10% (about 945L) shifted the calculated HRT significantly and the intercept of the median flow-export relationship. We also tested the assumption that saturated volume in the bioreactor remains constant in time. We back calculated the water depth from the flowrate and applied it to the surface area of the bioreactor to estimate volume at each time step. This effect on median HRT is small overall (average increase of 0.4 h), but the difference is larger at higher median HRTs. The difference between the saturated volume calculations was barely detectable in total nitrate export results.

Conclusion

To explore the impact of varying flow rates on bioreactor performance, we developed 100 scenarios using the gamma function to alter the shape of the distribution of flow rates. Scenarios ranged from a large number of low flow events to a small number of high flow events. We used a zero-order model to predict outflow nitrate concentration from hydraulic retention time. The TNE, a sum of all N export records in each scenario differed across the scenarios and decreased linearly with number of non-zero flow events. That is, a scenario with a few high flow events with high incoming loads of nitrate generated greater TNE than a scenario with frequent low flow events. This finding supports the general design practice of building the bioreactor with enough size and flow control to maintain a low flow rate. Further work on incorporating temperature impacts and modeling concentration-discharge relationships would improve the usefulness of

this type of analysis in designing field denitrifying bioreactors.

LITERATURE CITED

Addy, K., Gold, A. J., Christianson, L. E., David, M. B., Schipper, L. A., & Ratigan, N. A. (2016). Denitrifying Bioreactors for Nitrate Removal: A Meta-Analysis. *Journal of Environment Quality*. http://doi.org/10.2134/jeq2015.07.0399

Christianson, L. E., Bhandari, A., & Helmers, M. J. (2012). A practice-oriented review of woodchip bioreactors for subsurface agricultural drainage. *Applied Engineering in Agriculture*, *28*(6), 861–874. http://doi.org/10.13031/2013.42479

Christianson, L., Bhandari, A., & Helmers, M. (2011). Potential Design Methodology for Agricultural Drainage Denitrification Bioreactors. In *World Environmental and Water Resources Congress 2011* (pp. 2740–2748). Reston, VA: American Society of Civil Engineers. http://doi.org/10.1061/41173(414)285

Ghane, E., Fausey, N. R., & Brown, L. C. (2015). Modeling nitrate removal in a denitrification bed. *Water Research*, *71*, 294–305. http://doi.org/10.1016/j.watres.2014.10.039

Heinen, M. (2006). Simplified denitrification models: Overview and properties. *Geoderma*, *133*(3–4), 444–463. http://doi.org/http://dx.doi.org/10.1016/j.geoderma.2005.06.010

Halaburka, B. J., Lefevre, G. H., & Luthy, R. G. (2017). Evaluation of Mechanistic Models for Nitrate Removal in Woodchip Bioreactors. *Environmental Science and Technology*, *51*(9), 5156–5164. http://doi.org/10.1021/acs.est.7b01025

Hassanpour, B., Giri, S., Pluer, W. T., Steenhuis, T. S., & Geohring, L. D. (2017). Seasonal performance of denitrifying bioreactors in the Northeastern United States: Field trials. *Journal of Environmental Management*, *202*, 242–253. http://doi.org/10.1016/j.jenvman.2017.06.054

Hoover, N. L., Bhandari, A., Soupir, M. L., & Moorman, T. B. (2016). Woodchip Denitrification Bioreactors: Impact of Temperature and Hydraulic Retention Time on Nitrate Removal. *Journal of Environment Quality*, *45*(3), 803. http://doi.org/10.2134/jeq2015.03.0161

Jones, C. S., Wang, B., Schilling, K. E., & Chan, K. sik. (2017). Nitrate transport and supply limitations quantified using high-frequency stream monitoring and turning point analysis. *Journal of Hydrology*, *549*(x), 581–591. http://doi.org/10.1016/j.jhydrol.2017.04.041

Lam, W. V., Macrae, M. L., English, M. C., O'Halloran, I. P., Plach, J. M., & Wang, Y. (2016). Seasonal and event-based drivers of runoff and phosphorus export through agricultural tile drains under sandy loam soil in a cool temperate region. *Hydrological Processes*, *30*(15), 2644–2656. http://doi.org/10.1002/hyp.10871

Moorman, T. B., Tomer, M. D., Smith, D. R., & Jaynes, D. B. (2015). Evaluating the potential role of denitrifying bioreactors in reducing watershed-scale nitrate loads: A case study comparing three Midwestern (USA) watersheds. *Ecological Engineering*, *75*(3), 441–448. http://doi.org/10.1016/j.ecoleng.2014.11.062

Pluer, W. T., Geohring, L. D., Steenhuis, T. S., & Walter, M. T. (2016). Controls Influencing the Treatment of Excess Agricultural Nitrate with Denitrifying Bioreactors. *Journal of Environment Quality*, *45*(3), 772. https://doi.org/10.2134/jeq2015.06.0271

Schmidt, C. A., & Clark, M. W. (2013). Deciphering and modeling the physicochemical drivers of denitrification rates in bioreactors. *Ecological Engineering*, *60*, 276–288. http://doi.org/10.1016/j.ecoleng.2013.07.041

Wade, A. J., Palmer-Felgate, E. J., Halliday, S. J., Skeffington, R. A., Loewenthal, M., Jarvie, H. P., … Newman, J. R. (2012). Hydrochemical processes in lowland rivers: insights from in situ, high-resolution monitoring. *Hydrology and Earth System Sciences*, *16*(11), 4323–4342. http://doi.org/10.5194/hess-16-4323-2012